Chemical Engineering Journal 460 (2023) 141838

Contents lists available at ScienceDirect

Chemical Engineering Journal

journal homepage: www.elsevier.com/locate/cej

Comparison of lead adsorption on the aged conventional microplastics, biodegradable microplastics and environmentally-relevant tire wear particles

Wei Huang [a,b], Jiaqin Deng [a,c], Jie Liang [a,*], Xinghui Xia [b,*]

[a] College of Environmental Science and Engineering, Hunan University and Key Laboratory of Environmental Biology and Pollution Control (Hunan University), Ministry of Education, Changsha 410082, PR China
[b] Key Laboratory of Water and Sediment Sciences of Ministry of Education, State Key Laboratory of Water Environment Simulation, School of Environment, Beijing Normal University, Beijing 100875, PR China
[c] College of Environmental Science and Engineering, Central South University of Forestry and Technology, Changsha 410004, PR China

ARTICLE INFO

Keywords:
Microplastics
Tire wear particles
Aging
Metal ion
Adsorption mechanism
Desorption

ABSTRACT

In this study, the adsorption behavior of lead (Pb(II)) onto environmentally-relevant tire wear particles (TWP) gained by natural weathering and mechanical abrasion, ultraviolet-aged polylactic acid microplastics (UV-PLA), and ultraviolet-aged polystyrene microplastics (UV-PS) was compared to investigate the difference of representative microplastics between the adsorption capacity and mechanism. Our results indicated that the aging processes significantly improved the adsorption capacity to Pb(II), and TWP had the highest adsorption amount, followed the order by UV-PLA, UV-PS, PLA and PS. Electrostatic interaction and complexation of oxygen-containing functional groups played crucial roles in the adsorption of Pb(II) onto UV-PLA, the adsorption mechanisms of UV-PS involved electrostatic interaction, complexation and cation-π interaction, while adsorption of TWP was might dominated by the complexation of surface functional groups and properties of the complex rubber co-polymer. Interestingly, the low concentration of humic acid (HA) most significantly improved adsorption capacity of aged microplastics to Pb(II), otherwise it was severely suppressed at higher concentration of HA. Besides, the adsorption behavior of different binary systems between aged microplastics and suspended sediment to Pb(II) had complicated synergistic or suppressive effects with a concentration-dependent and polymer-dependent trend. Furthermore, UV-PLA had the far stronger desorption ability of Pb(II) than that of TWP and UV-PS, suggesting that metal-contaminated biodegradable microplastics posed the higher ecological risks to aquatic organisms. Desorption quantity and rates of Pb(II) from aged microplastics in the simulated sediment system were generally higher than those in turbulent water column. Collectively, these findings provide a wide insight into adsorption capacity and mechanisms of metal ions on the representative aged microplastics and the desorption behavior in complex aquatic environments.

1. Introduction

Due to the advantages of low cost, simple manufacturing process, stable physicochemical properties, strong durability and adaptability, the global annual production of plastics (mostly conventional non-degradable petroleum-based plastic materials) has increased rapidly in recent decades and reached almost 368 million tonnes (Mt) in 2019 from 359 Mt in 2018 [1]. However, because of the overuse, mismanagement and environmental durability of plastic products, about 6300 Mt plastic wastes had been continuously produced from 1950 to 2015, 79 % of which was released into landfills or natural environments [2]. The plastics in the natural environments can be gradually fragmented into microplastics (size <5 mm) via the environmental weathering and extremely slow biodegradation for a long period [3,4]. On the other hand, countless primary microplastics (e.g., microbeads in consumer products, industrial abrasives, accidental plastic pellets, microfiber from textiles and fishing nets) were also discharged into the environments [5,6]. Microplastics are everywhere including ocean, freshwater, terrestrial environments and atmosphere, and the conceptual model of the “microplastic cycle” similar as a biogeochemical cycle has been put

* Corresponding authors.
E-mail addresses: liangjie@hnu.edu.cn (J. Liang), xiaxh@bnu.edu.cn (X. Xia).

https://doi.org/10.1016/j.cej.2023.141838

Available online 11 February 2023

forward by scientists [7,8]. Microplastics, as an ubiquitous, diversified and complex contaminants, cause detrimental effects on biosphere and human health and raised global concern [9,10].

Bioplastics including bio-based, biodegradable or both properties of plastics mainly derived from "green" and renewable raw material and can be entirely decomposed into low molecular weight compounds such as water and carbon dioxide by microbials, which can ease the supply of petroleum resource and be centralized composting biochemical disposal under appropriate conditions [11,12]. As a promising alternative to conventional non-degradable polymers (mostly petroleum-based plastics), bioplastics or biodegradable plastics have received extensive attention in recent years [13]. Common bioplastics include biodegradable polylactic acid (PLA), polyhydroxybutyric acid, polybutadiene and starch blends; non-degradable bio-based PE, PP and PET; fossil-based but biodegradable polyadipate dipolybutylene terephthalate (PBAT) [12,13]. Biodegradability of bioplastics can be significantly influenced by the polymer structure itself, additives, and biotic and abiotic factors such as environmental media, ultraviolet light, temperature, pH, humidity, salinity, microbial abundance and enzyme activity [14]. Thus, the ideal rapid degradation conditions of bioplastics are often not achieved under the realistic environment and it can thus exist for an unpredictable time. Recent evidence has showed that the formation of microplastics and even nanoplastics from bioplastics or biodegradable plastics in natural environments is a persistent process [15–17]. Similar with conventional microplastics, ecologists found that biodegradable microplastics (e.g., PLA, polyhydroxybutyrate) and associated chemicals (e.g., additives) had different adverse impacts on aquatic organisms (e.g., lugworm *Arenicola marina*, European flat oyster *Ostrea edulis*, blue mussel *Mytilus edulis*, zebrafish *Danio rerio*, freshwater oligochaete *Lumbriculus variegatus*, green alga *Chlamydomonas reinhardtii* and crustacean *Daphnia magna*), and potentially affected biogeochemical cycling and ecological functions in the aquatic environment [16,18–20]. The exposure of PLA microplastics (2.34 ± 0.07 μm) at an environmentally relevant concentration caused an adverse effects on the growth and development of amphibian *Physalaemus cuvieri* tadpoles and showed the neurotoxic action [21]. Since the majority of research focused on the conventional non-degradable microplastics, the adsorption behavior of biodegradable microplastics and toxic metal ions and their combined impacts to aquatic organisms remain limited.

On the other hand, TWP was regarded as a class of representative microplastics due to its extremely complex mixture composition such as rubber/elastomer, reinforcing fillers, vulcanization agents, textile & metal net, and various additives, and gained extensive concern in recent years because of its widespread, durability and toxicity [22,23]. TWP, which was generated from mechanical abrasion and brakes of tire materials during automobile traffic and divided into airborne and non-airborne emissions, can be widely released into road side, soils and aquatic environments (especially urban waters) with at least million tons emission flux per year through the atmospheric transport and surface runoff [22,24]. Up to now, the ecotoxicological effects of TWP have been proved that adverse effects on aquatic biota (e.g., microalgae, benthic macroinvertebrates, mussels, fish) can be caused by the TWP ingestion and chronic effects [25], as well as through the exposure of toxic leachate (e.g., Zn, organic additives) released from TWP [26,27]. Furthermore, Fan *et al.,* reported the adsorption of heavy metals (Cd(II) and Pb(II)) and antibiotics by TWP with an artificial ultraviolet aging treatment and showed that UV-TWP have a certain adsorption capacity [28,29]. Nevertheless, the adsorption mechanisms of these environmental pollutants onto TWP and the effects of leaching metal ions on adsorption are largely unclear. Moreover, there is lack of study about the adsorption behavior of environmentally-relevant TWP to chemical contaminants.

Owing to its environmental persistence, mobility, and unique physicochemical properties (e.g., particle size, large specific areas, pore structure, hydrophobicity, surface functional groups), conventional petroleum-based microplastics represent an anthropogenic vector for various toxic metal ions in the aquatic environment and pose a great environmental threat [30,31]. Furthermore, the environmental weathering/aging processes (e.g., physical abrasion, heat, UV irradiation, chemical oxidation, biofilm attachment or biodegradation) can significantly affect the physicochemical characteristics of microplastics, and might alter their fate, transport and sorption behavior [32,33]. The adsorption properties of aged conventional microplastics (e.g., PS, PE, PVC, PET) have been widely conducted and it generally showed the greater adsorption ability to metal ions than the pristine one [34,35]. Field investigations showed that the trace metals (e.g., Pb(II), Cu(II), Cd (II), total Cr, Ni(II), Zn(II), Total Mn) at the 0-μg/g level were presence in the naturally-aged microplastics collected from wild aquatic environments (e.g., freshwater, oceans, estuaries) [36,37], indicating that microplastics have the potential to adsorb toxic metals and the level of attached metals might be location-dependent [38]. Sometimes, the heavy metal contents on the surface of microplastics were even higher than that of surrounding media (e.g., sewage sludge, sediments) [30,39]. Microplastics and absorbed metal pollutants can generate ecotoxicological effects to aquatic organisms, transfer through the food chain and even pose nonnegligible risks to human health [9]. Nevertheless, compared with the conventional petroleum-based microplastics, the environmental adsorption behavior and mechanisms of aged biodegradable microplastics and TWP to metal ions and associated environmental impacts have gained less attention and is required to further explore [40].

Considering the complexity of actual aquatic environment especially seawater, urban natural waters and wastewater treatment plants, the physicochemical properties and related adsorption–desorption behavior of microplastics may be affected by realistic environmental factors and media. For example, pH can affect the surface charges of microplastics in solution and then change their electrostatic interactions with metal ions [41]. Humic substrates, which is a common and ubiquitous natural organic matters with the negatively charge and has abundant oxygen-containing functional groups (e.g., aromatics, hydroxyl groups and phenolic groups), can be regarded as an important factor in the adsorption behavior of materials [42]. Moreover, salinity condition represents the environmental differences between freshwater, estuary, ocean and its boundaries, and thus should be considered in the microplastic study [43]. Due to the various contaminants (e.g., metal ions, organic pollutants) co-existing in aquatic environments, they may be simultaneously absorbed by microplastics. In addition, several studies reported the effects of surfactants and suspended sediments on transport behavior of microplastics in the aquatic media [44,45], while its impacts on the microplastic adsorption behavior remain unclear. On the other hand, desorption process plays a significant role in influencing the fate, bioavailability and ecological risks of chemical pollutants absorbed onto microplastics in the aquatic environment [46,47]. Therefore, scientific assessment of the effects of environmental conditions (e.g., HA, salinity, exposure media) on adsorption–desorption of metal ions on aged microplastics is crucial.

Lead (Pb(II)), which is considered as one of the most toxic metal ions owing to its solubility, mobility, acute toxicity and bioaccumulation, widely spread over aquatic surroundings and always accumulate on the microplastic surfaces [36,37]. The polystyrene polymer was selected to delegate the conventional non-degradable microplastics, because it is one of the largest amounts of plastic products and has been widely detected in various aquatic environments [1]. Conventional petroleum-based microplastics can serve as an anthropogenic "vector" of various toxic contaminants in the aquatic environment, but little is known about the adsorption–desorption of biodegradable microplastics and environmentally-relevant TWP to metal ions. Consequently, in this work, the objectives are (1) to compare Pb(II) adsorption ability of TWP, UV-PLA, UV-PS, PLA and PS, and reveal their underlying adsorption mechanisms; (2) to comprehensively investigate the effects of aquatic environmental factors (pH, HA, salinity, surfactant, coexistence metal ion) and particle components (suspended sediment) on the adsorption

behavior of Pb(II) onto three representative aged microplastics (TWP, UV-PLA, UV-PS); and (3) to contrast the desorption capacity of Pb(II) from three aged microplastics in simulated aquatic components (sediment and turbulent water column) and explore the effects of environment factors (HA and salinity) on desorption behavior.

2. Materials and methods

2.1. Materials and reagents

Commercial pristine polystyrene (PS) and biodegradable polylactic acid (PLA) particles both without plastic additives, with a marked diameter of 100 mesh, were purchased from Dongguan Jing Tian Raw Materials of Plastics Co., ltd. (Guangdong, China). The two types of microplastics were cleaned with ultra-pure water and then air dried at low temperature, respectively. Two worn old car tires (Michelin) were friendly provided by a TIREPLUS Automobile Service Center in the Yuelu District (Changsha, China). The detailed information about worn car tires was noted in Table S1. To simulate the effect of suspended sediment (SPS) on sorption process, surface sediment samples (0–5 cm depth) were collected from an urban river, Xiangjiang River (Changsha, China). The information about collection, preparation and properties of sediment was provided in Table S3.

Lead nitrate, cupric nitrate, sodium chloride (NaCl), sodium dodecyl sulfate (SDS) and nitric acid (HNO_3) were obtained from Sinopharm Chemical Reagent Co., ltd. (Shanghai, China). All chemical reagents were analytical pure grade. Humic acid ($C_9H_9NO_6$, fulvic acid $\geq$90 %) was purchased from Macklin Co., ltd. (Shanghai, China). All solutions were prepared using ultra-pure water (18.25 ΩM). Metal stock solutions of 1000 mg/L were prepared and used to the following adsorption experiment.

2.2. Sample preparation and characterization of aged microplastics

It is well known that studies on the pristine microplastics are environmentally irrelevant, because its nature "weathering" processes (e.g., heat, mechanical abrasion, ultraviolet radiation, biofilm attachment and biodegradation) accompanied by the polymer physicochemical change are inevitable. Herein, ultraviolet photo (UV) radiation was chosen for aging the conventional and biodegradable microplastics in the aquatic environment due to photoaging of plastics as a typical natural weathering process [48,49]. The PLA and PS microplastics were put into a photochemical reaction instrument (BL-GHX-V, BiLon corporation, China) equipped with a 1000 W Hg lamp (λ of the full spectrum, γ_{max} = 365 nm, 20000 μW/cm^2) for 12 to 144 hour (h) UV radiation exposure, respectively. Microplastics at the different UV-aging time point including 12, 24, 48, 72, 144 h were characterized and contrasted. According to the aging result of our preliminary experiment, microplastics undergoing for 144 h UV-aging were selected as the aged samples in the following adsorption experiments and characterization. The detailed information was documented in the supporting information Text S3.

For simulating the environmentally relevant scenario of car tire particles exposure, two worn old tires (Michelin) were subjected to a series of mechanical abrasion treatments and finally TWP were gained (Fig. S1). Using a metal grater, micrometer sized TWP were scrapped from 1 cm of the external surface of each worn old tire. The detailed steps for obtaining the environmentally-relevant TWP were noted in the supporting information Text S3. Considering the potential effects of leaching Pb(II) on adsorption experiment, the metal release kinetics from TWP was investigated for a week and metals were recorded in Table S4. The leaching system was composed of a solid-to-liquid ratio of 20 mg TWP per 20 mL ultra-pure water, which is consistent with the adsorption system. Then, the filtrate was detected by the inductively coupled plasma mass spectrometry (7900 ICP-MS, Aglient Instrument Co., ltd., USA).

To comprehensively evaluate the variation of physicochemical properties of microplastics after aging process and reveal their adsorption mechanism, a series of typical characterization methods have been applied. The surface morphologies and energy spectra were observed by field emission scanning electron microscope (FEI Nova Nano SEM 230, USA) and its matched energy-dispersive X-ray spectroscopy (EDS), respectively. The Brunauer-Emmett-Teller (BET) specific surface area and pore distribution were measured by surface area and porosity analyzer (Micromeritics, ASAP 2020 PLUS HD88, USA) with the N_2 adsorption–desorption analysis method. The water-phase diameter was measured by laser particle analyzer (Malvern Mastersizer 2000, UK). The Zeta potential was determined by the Malvern Zetasizer Nano ZS (UK). The detailed measurement methods of diameter and Zeta potential of microplastics were provided in the Supporting information Text S5. The water contact angle was observed by contact angle measuring instrument (JC2000D1, Shanghai Zhongchen digital technic apparatus co., ltd, China). The crystallographic structure was obtained by X-ray diffraction (XRD) performed on Bruker advance D8 in the range of $10^\circ \leq 2\theta \leq 80^\circ$ (Bruker, Germany), and the crystallinity was simulated by MDI Jade V6.0 software. Furthermore, Fourier transform infrared spectroscopy (FT-IR) and X-ray photoelectron spectroscopy (XPS) were applied to determine the surface functional group compositions of microplastics. The FT-IR spectra were detected in the 4000–400 cm^{-1} region with a resolution of 4 cm^{-1} by a Microscopy-Fourier transform infrared spectrometer (NICOLET iN10 FT-IR, Thermo Scientific Co., ltd, USA). The XPS information was gained by an X-ray spectrometer (K-Alpha, Thermo Fisher Scientific Inc., USA) and the spectra were analyzed using XPS Avantage software. In order to further evaluate the chemical aging degree of microplastics, the carbonyl index and oxygen/carbon atom ratio of UV-PLA and UV-PS was calculated by the methods in the supporting information Text S6.

TWP, a type of complex mixtures (including rubbers, fillers, reinforcement agents, processing aids, accelerators and retarders, adhesives, and activators) with the elastomer property [22], can not be well characterized by the conventional FT-IR spectroscopy due to the composition complexity and elastomer characteristics of material itself, according to our observation results. The optical-photothermal infrared microspectroscopy (O-PTIR), with the advantage of visualization, high spatial resolution (roughly 400 nm), excellent sensitivity (roughly 0.4 pg) and anti-fluorescence interference, is an emerging technique and has been applied to submicrometre-resolved imaging of individual particles and firstly determined the chemical properties of polydimethylsiloxane elastomer microplastics [50]. In this study, TWP samples were determined by a mid-IR (1800–800 cm^{-1}) O-PTIR microspectroscope (Photothermal Spectroscopy Co., ltd). By locating the sampling area (50 × 50 μm^2), imaging and spectra of TWP sample surface was observed.

2.3. Batch adsorption experiments

The potential of five representative microplastics (UV-PLA, PLA, UV-PS, PS and TWP) as vector of metal ions was investigated. Adsorption experiments were conducted in 50 mL glass conical flasks in the dark at 25 °C in the water-bath thermostatic shaker (SHY-2A, Changzhou Guoyu Instrument ltd., China). The adsorption kinetics of microplastics were accomplished with a solid-to-liquid ratio of 20 mg per 20 mL (mass: volume = 1 g/L), and the initial Pb(II) concentration was 10 mg/L at pH of 5.0 ± 0.1. The solution pH was selected to avoid the precipitation of metal oxides in the Pb(II) solution [51]. All the glass vials were shaken at 160 rpm, and the solutions were passed through a 0.22 μm PES filter membrane. The shake times ranged from 0.5 to 48 h, and the results suggested that 48 h was sufficient to reach the adsorption equilibrium.

A batch adsorption isotherm experiment was performed in same experimental conditions with the adsorption kinetics. In the isotherm experiment, the solid-to-liquid ratio was 20 mg of microplastics per 20 mL of background solution. Pb(II) solution with the different concentration was gained by diluting the stock solutions (1000 mg/L) with ultra-pure water and adjusted pH with 0.1 mol/L HCl and 0.1 mol/L

NaOH. The solutions containing a wide range of initial Pb(II) (1–30 mg/L) were set to obtain adsorption equilibrium concentrations. All 50 mL glass conical flasks were shaken at 160 rpm in a dark condition at 25 °C for 48 h. The filtered solution samples were acidified with HNO_3 occupied 0.1 % of the total volume and then Pb(II) concentrations in the filtrates were measured by an inductively coupled plasma optical emission spectrometer (Avio 500 ICP-OES, PerkinElmer Instrument Co., ltd, USA). Eventually, five types of microplastics were respectively washed by ultra-pure water to remove surface residual metal ions, and then air dried at 30 °C for the following characterization and desorption experiment.

Given that the complexity of aquatic environments and presence of microplastics in the aged form, subsequent works were carried out to investigate the effects of aquatic chemistry including pH, HA, salinity, surfactant, metal ion coexistence and SPS at environmentally relevant concentrations on the adsorption behavior of Pb(II) onto three representative aged microplastics (TWP, UV-PLA and UV-PS). To investigate the effects of pH values, pH of 20 mL Pb(II) solution (10 mg/L) was were adjusted to between 4.0 and 7.0 using 0.1 mol/L NaOH and 0.1 mol/L HNO_3. Then, Pb(II) solution with different pH value was used in adsorption experiments to determine the pH value and Pb(II) concentration in the solution after reaching adsorption equilibrium of 20 mg aged microplastics (mass: volume = 1 g/L). To study the effects of humic substrates and salinity, the adsorption systems of aged microplastics were performed with 10 mg/L Pb(II) solution containing different concentrations of HA (0, 1, 10, 20, 50 mg/L) or NaCl (0, 10, 50, 200, 500 mM). These concentrations of HA and NaCl represent the actual level in various aquatic environments such as fresh water, seawater and their intersections [45]. To examine the impacts of surfactant on the Pb(II) adsorption onto aged microplastics, same experimental procedure was conducted in the 20 mL Pb(II) solution (10 mg/L) with the addition of sodium dodecyl sulfate (SDS, 0, 1, 10, 20, 50 mg/L). Due to the ubiquity of Cu(II) in the aquatic environment and its ease of adsorption onto microplastics [34], the effects of co-existing Cu(II) (0, 0.5, 1, 5, 10 mg/L) on the Pb(II) adsorption process were explored. Furthermore, the environmentally-relevant suspended sediment concentration (SPS, 0, 1, 10, 100, 500 mg/L) was selected as the representative concentration to investigate the effects of SPS on Pb(II) adsorption by aged microplastics [52]. After reaching adsorption equilibrium, the superficial mixture in the solution was filtered, collected and air dried, and the morphology of microplastics-sediment combination mixtures was observed using the scanning electron microscope.

2.4. Desorption experiments of Pb(II)-laden aged microplastics

The initial adsorbed concentration of Pb(II) was 10 mg/L, and three types of aged microplastics reaching Pb(II) adsorption equilibration for 48 h, named Pb-laden UV-PLA, Pb-laden UV-PS and Pb-laden TWP, were collected and air-dried in 30℃. Herein, the desorption behavior of Pb (II)-laden aged microplastics in two aquatic environments (sediment environment and turbulent water column) was performed, respectively. On the one hand, 0.01 mol/L $CaCl_2$ background solution (pH = 6.0 ± 0.1) was used to simulate the desorption process in the sediment environment [41]. Due to preliminary experiments showing 48 h desorption equilibrium, 20 mg of Pb(II)-laden aged microplastics were added to 20 mL of background solution, and mixture was oscillated at 160 rpm in a dark condition at 25 °C. On the other hand, the desorption behavior of Pb(II)-laden aged microplastics in the turbulent water column was simulated by solution ultrasonication. 20 mg Pb(II)-laden aged microplastics was added into 20 mL of ultra-pure water (pH = 5.0 ± 0.1) as the background solution and then 50 mL conical flask was put into an ultrasonic cleaning machine (KQ5200E, 40KHz, 200 W, Kunshan Ultrasonic Instrument Co., ltd, China) for 30 min in a dark environment at room temperature. Subsequently, the filtrate was filtered by a 0.22 μm PES filter membrane and measured by the 7900 ICP-MS (Aglient Instrument Co., ltd., USA). Each treatment was performed in triplicate.

In order to examine the influence of environmental factors on the desorption behavior of three Pb(II)-laden aged microplastics, the desorption process in the presence of HA (10 mg/L) or salinity (NaCl, 50 mM) was studied in the simulated sediment environment and turbulent water column, respectively. A series of experimental groups in the sediment environment or turbulent water column was set up as follow: Pb(II)-laden aged microplastics, Pb(II)-laden aged microplastics + HA (10 mg/L), and Pb(II)-laden aged microplastics + NaCl (50 mM), respectively. The experimental operation with the addition of environmental factors was in accordance with the above experimental procedure.

2.5. Quality control

To avoid the environmental interference from potential impurities and cross-contamination, all experimental procedures were performed in a clean laboratory with no more than two participants. Participants must wear cotton-made lab coat and nitrile gloves. In addition, all glass wares used in the experiment were soaked in 5 % (v/v) HNO_3 solution for more than 24 h and then thoroughly washed three times with the ultra-pure water. Importantly, blank calibration controls (without the addition of microplastics) were conducted in triplicate for each concentration of metal ions in this work. Considering the loss caused by adsorption onto the glass ware surface, the real solute concentrations in the blank calibration controls were measured after 48 h equilibrium. Finally, the solute adsorbed onto microplastics was calculated by subtracting the concentration of corresponding filtrates from its blank controls. The measurements of the blanks and calibration controls were performed in triplicate and data values represent mean ± standard deviation (n = 3).

2.6. Data analysis

The pseudo-first-order kinetic model, pseudo-second-order kinetic model, interparticle diffusion model and film diffusion model were used to fit the kinetics of Pb(II) adsorption onto microplastics, while the Langmuir and Freundlich models were applied to fit the adsorption isotherms. The detailed information of these models and related equations was documented in Table S5. The OriginPro 2021 software was used to perform the fitting of above adsorption model, whose fitting parameters were listed in the Supporting Information. The significance of the parameters was tested at $p < 0.05$, following one-way analysis of variance (ANOVA). In addition, desorption rate (%) was ratio of Pb(II) amounts desorbed from Pb(II)-laden aged microplastics to the Pb(II) amounts absorbed onto microplastics.

3. Results and discussion

3.1. Characterization of the representative microplastics

3.1.1. Evaluating changes in physical properties of aged microplastics

With the UV-aging process from 0 to 144 h, the exterior color of PS and PLA microplastics gradually turned to yellow, especially UV-PS microplastics (Fig. S2), indicating that the surface of pristine microplastics suffered from different degrees of photo-oxidation/degradation. The main reason might be that the unsaturated chromophoric groups of microplastics were degraded by UV radiation [53]. As for the TWP gained by natural weathering and mechanical abrasion, it still showed a black color similar with the normal car tires (Fig. S2). SEM images showed that the microcosmic surface changes of representative microplastics after aging (Fig. 1), and explained the physic damage of plastic polymer structure caused by UV photooxidation/degradation. Notably, the UV-PLA microplastics exhibited the obviously irregular and rougher surface with a series of cracks, pits and bumps, and formation of the smaller broken particles (Fig. 1b). In addition, by the comparative anlysis of particle size distribution of PLA and PS before and after UV-aging,

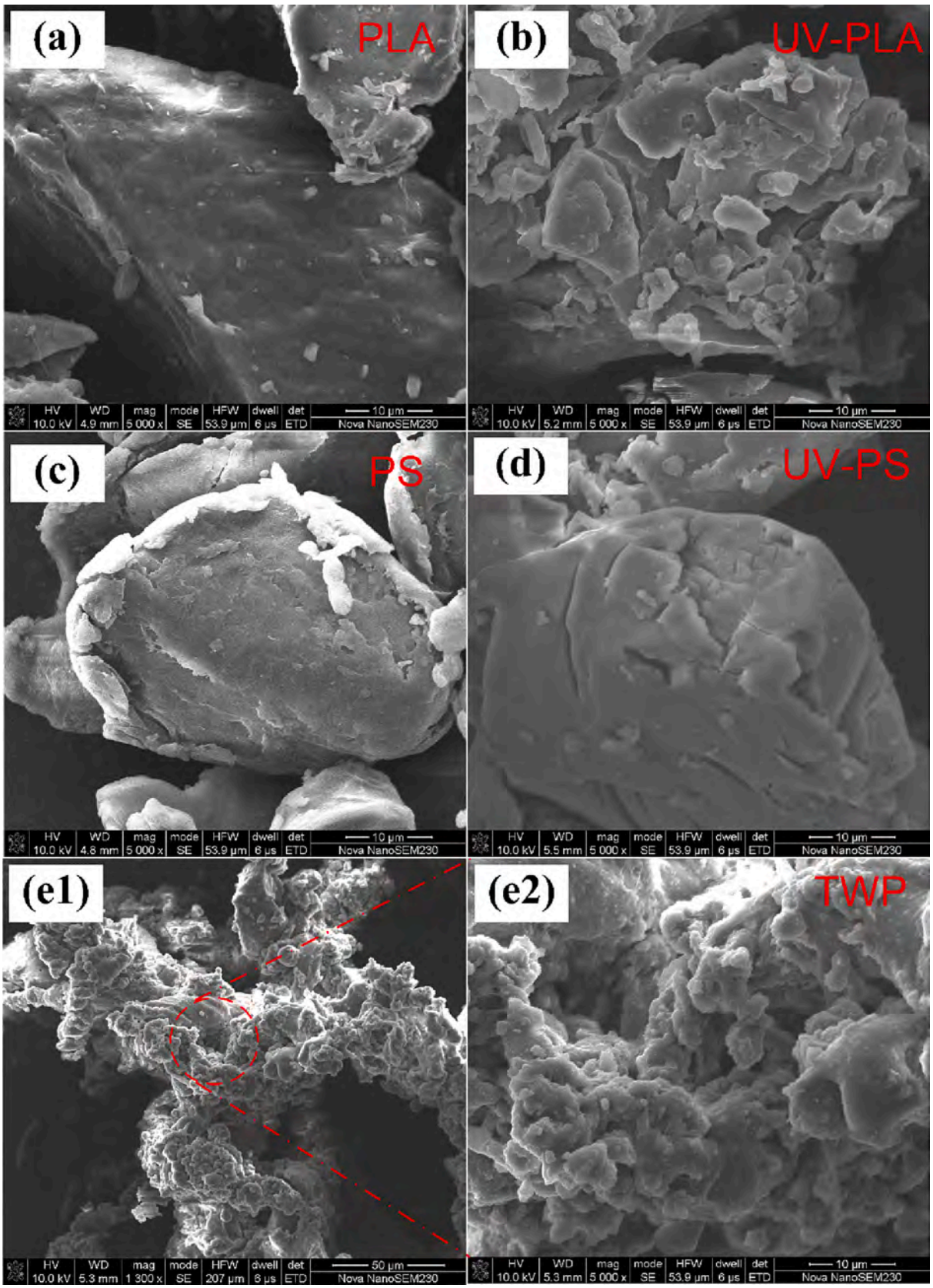

Fig. 1. SEM images of the microcosmic surface structure of (a) PLA, (b) UV-PLA, (c) PS, (d) UV-PS and (e) TWP.

results showed that PLA microplastics are broken in the process of UV radiation with the formation of smaller plastic particles (Table 1 and Fig. S3), whose phenomenon was consistent with the aboved-mentioned SEM results. Similarly, recent studies reported the "greenwashing" fact that the claimed biodegradable commercial plastic products including PBAT films and sheets, polyhydroxybutyrate particles, poly(p-dioxanone) films, PLA films, mineral doped polyethylene fims, PLA blend films and PBAT blend films did not degrade quickly in the natural environment, otherwise they were more likely to break into microplastics and even nanoplastics than the conventional plastics such as LDPE film strips, PET bottles and PVC tubes [15–17]. Therefore, biodegradable plastics or microplastics showed the weaker resistance than conventional plastics, which may be related to the difference of chemical composition and anti-aging ability of plastics. Furthermore, the multiple risks from biodegradable microplastics was nonnegligible and required to be further assessment with regards to the longer transformation, formation of secondary micro/nanoplastics, and its ecotoxicological effect of intermediate products and final products to the natural surroudings and various organisms.

In Fig. 1e and Fig. S2, SEM images exhibited the serious rough and fluffy surface structure of TWP gained by natural aging and mechanical abrasion, and EDS analysis represented the main composition of carbon (C), oxgen (O), Zn, and Pb. Besides, the specific surface area values of UV-PLA, PLA, UV-PS, PS and TWP was 15.37, 4.91, 5.62, 3.16 and 3.84 m^2/g, respectively, and their total pore volume varied from 0.0016 to 0.012 cm^3/g (Table 1). Thle results implied that environmental aging process can significantly increase the surface area and pore volume of microplastics, but these two property values of TWP are still small. In Fig. 2a and 2b, the water contact angle of pristine PS microplastics decreased from 91.9° to 81.4° after aging, indicating UV-PS with a relatively hydrophilic surface, whereas biodegradable PLA miroplastics before and after aging all showed tiny contact angles and suggested the strong hydrophilcity, due to its raw materials derived from biomass. The differences in water contact angle ware mainly attributed to the changes of surface oxygen-containing functional groups. In addition, the Zeta potential values of five types of microplastics were getting more negative as the increase of pH value from 2 to 10 (Fig. 2c). Notably, aged microplastics, especially UV-PLA, generally showed a more negative Zeta potential than the pristine microplastics in any same solution pH value, suggesting that aging processs can significanty increase the surface anions of aged microplastics. Moreover, the XRD spectra of UV-PLA, PLA, UV-PS, PS and TWP exhibited in Fig. 2d, and these peaks indicated that microplastics have a certain crystallinity. However, from the view of plot, there was no significant change in the crystal structure of PLA and PS after aging process, which was consistent with previous studies [54]. To further investigate the potential effects of aging, the crystallinity of UV-PLA, PLA and TWP was gained with 16.52 ± 1.04 %, 3.93 ± 0.54 % and 2.50 ± 0.12 % based on the calculation of MDI Jade V6.0 software, but crystalline structure of PS and UV-PS might be so poor that it was not calculated (Table 1).

3.1.2. Evaluating changes in chemical properties of aged microplastics

FT-IR spectra showed that, after UV-aging 12, 24, 48, 72, 144 h, typical peaks were presented at 1392, 1700–1800, 2940–2960, 3420 cm^{-1} for UV-PLA, and at 698, 756, 1029, 1450, 1601, 2923, 3023 cm^{-1} for UV-PS (Fig. 3a and 3b). For UV-PLA, the characteristic absorption peak at 1700–1800 cm^{-1} was assigned to carbonyl group (C═O). Also, the 3432 and 2940–2960 cm^{-1} was peak of hydroxyl group stretching vibration (O—H) and methylene (–CH_2) in UV-PLA, respectively. For UV-PS, the absorption peak at 1450, 1601 and 2923 cm^{-1} was assigned to stretching vibration of C═O, aromatic and –CH_2, respetively. Besides, these peaks at 698, 756 and 1029 cm^{-1} are the stretching vibration of the aromatic C—H bond on the benzene ring [55]. In comparison to UV-PLA and UV-PS, the above results demonstrated the differences of functional group species (e.g., specific aromatic structure in UV-PS) and strength of absorption peaks (e.g., abundant C═O and O—H in UV-PLA), indicating that biodegradable microplastics showed the different chemical structure (e.g., element content, functional groups) with the conventional non-degradable microplastics.

Furthermore, carbonyl index was normally used to characterize the chemical aging degree of plastics, which was calculated by the intensity of carbonyl relative to the methylene peak (1700–1800/2940–2960 for UV-PLA and 1450/2923 for UV-PS, respectively). As shown in Fig. 3c, the carbonyl index values of UV-PLA and UV-PS aging from 0 to 144 h is from 1.168 to 2.094 and 0.231 to 0.326, respectively. The carbonyl index values were markedly dependent upon the types of UV-PLA and UV-PS, revealing that the inherent structures of microplastic polymer affected their aging properties. Forward, the correlation analysis between carbonyl index and aging time of PLA and PS microplastics was investigated. The carbonyl index of PLA and PS versus aging time followed a significant linear correlation (r^2 = 0.990 and 0.961 for UV-PLA and UV-PS, respectively). Notably, the slope of correlation analysis between UV-PLA and UV-PS was 0.00641 and 0.000624, clearly suggesting that PLA microplastics more easily suffered from photo-oxidative degredation and fragmentation than the PS. This result was also evidenced by the SEM morphology and particle size distribution of UV-PLA after UV-aging 144 h (Fig. 1 and Fig. S3). Additionally, the increasing carbonyl index of UV-PLA and UV-PS with the increasing aging time indicated that UV-aging enhanced the formation of oxygen-containing functional groups especially C═O and destoryed the carbon chain and bond, which was consistent with the analysis of water contact angle and changes of hydrophilicity of aged microplastics (Fig. 2a and 2b). This phenomenon might be attributed to the availability of active sites on microplastic surfaces because the free radicals in the artificial aging simulation system was produced continuously under UV radiation, which can explain the linear increase of the O/C ratio in the aging period [56]. In the natural environment, weathering processes of microplastics probably exhibited a similar phenomenon on surface chemical properties due to the ubiquitous and continuous sunlight or chemical aging [57].

In addition, oxygen/carbon (O/C) atom ratio was an alternative indicator of carbonyl index to evaluate the aging degree of microplastics [58]. To clearly evaluate the aging degree of PLA and PS microplastics after UV-aging 144 h, we calculated the O/C ratio according to the XPS analysis results and compared their O/C ratio value with the TWP. As exhibited in Table 1, the order of O/C ratio values in UV-PLA, PLA, UV-

Table 1
BET-N_2 specific surface area (SA), total pore volume (V_{total}), particle diameter distribution, crystallinity and oxygen/carbon ratio of UV-PLA, PLA, UV-PS, PS and TWP.

Properties		UV-PLA	PLA	UV-PS	PS	TWP
SA (m^2/g)		15.37	4.91	5.62	3.16	3.84
V_{total} (cm^3/g)		0.012	0.0062	0.0054	0.0029	0.0016
Particle diameter distribution (μm)	D[4,3]	44.93	93.74	59.63	64.63	101.62
	D[4,3]	24.19	46.78	33.88	36.77	93.48
	D(V,0.1)	12.47	24.32	21.78	23.48	65.57
	D(V,0.5)	37.65	76.76	53.86	57.64	99.09
	D(V,0.9)	89.03	191.22	107.20	116.90	141.67
Crystallinity (%)		16.52 ± 1.04	3.93 ± 0.54	Not calculated	Not calculated	2.50 ± 0.12
Oxygen/carbon ratio		0.441	0.380	0.143	0.010	0.030

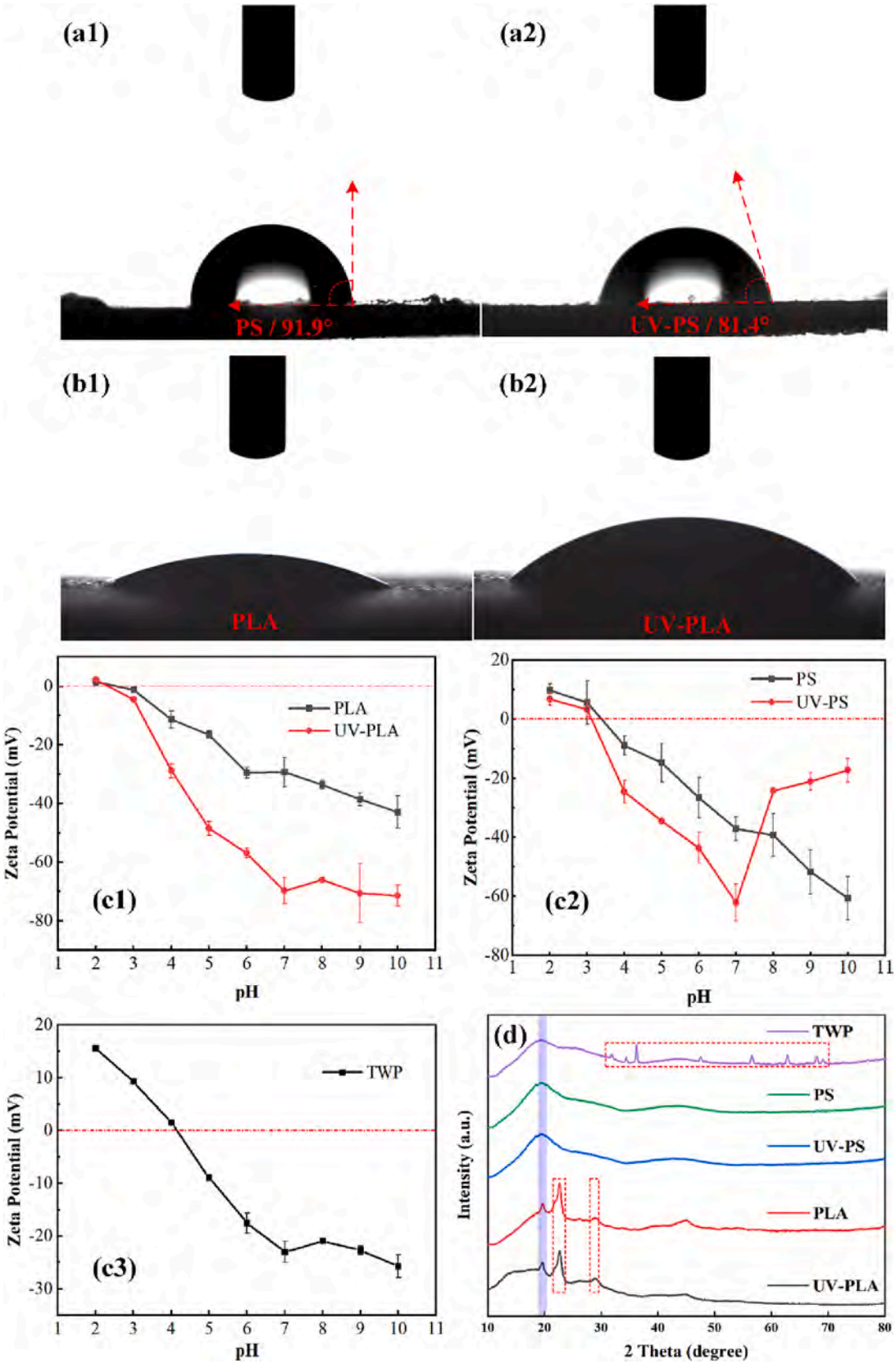

Fig. 2. Water contact angle of (a) PS and UV-PS, (b) PLA and UV-PLA; Zeta potential of (c1) PLA and UV-PLA, (c2) PS and UV-PS, and (c3) TWP; (d) XRD spectra of UV-PLA, PLA, UV-PS, PS and TWP.

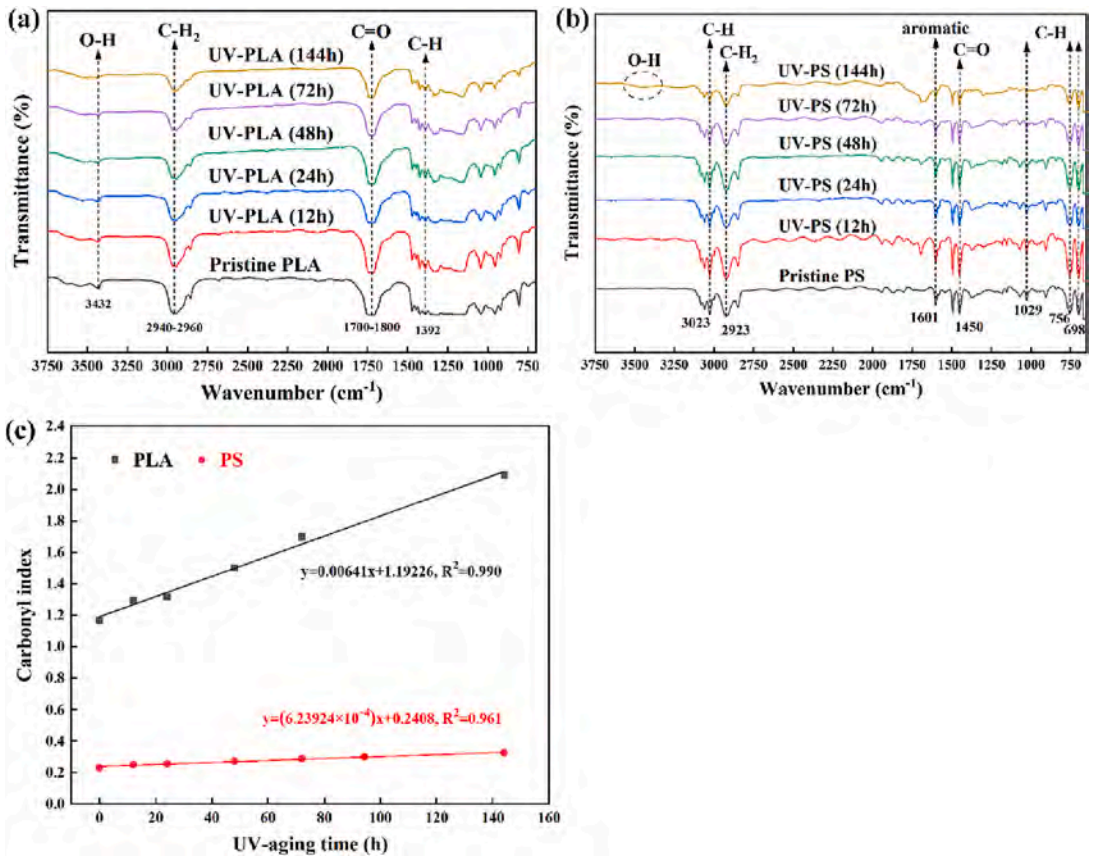

Fig. 3. FT-IR spectra of (a) UV-PLA and (b) UV-PS aging from 0 to 144 h; (c) Correlation analysis diagram between carbonyl index and aging time of PLA and PS microplastics.

PS and PS was followed by 0.441, 0.380, 0.143 and 0.010, pristine or aged PLA microplastics of which was larger than the PS microplastics regardless of the UV aging. In contrast, O/C ratio value of the TWP was 0.030, reflecting that its surface oxygen-containing functional groups is not abundant. Our results indicated that the O/C ratio was significantly relied on the types of microplastic polymer, which was similar to carbonyl index analysis. In comparison with the pristine microplastics, the O/C ratio of aged microplastics both showed a slightly rising trend. Nevetheless, the O/C ratio growth trend of UV-PLA was slower than the UV-PS, which showed a different result with the slope of the correlation analysis between carbonyl index and aging time mentioned above. The observation may be attributed to the difference between XPS and FT-IR techniques, where XPS allows for a nanometer-thick surface analysis, while FT-IR probes the micrometer depth.

Because the oxidation reaction was initiated from the polymer surface, a longer time was required for the interior oxidation of microplastics. The easier operation and lower costs of the FT-IR technique enabled the wide application of carbonyl index for characterizing polymer aging. However, natural aging processes, especially UV irradiation, were primarily confined to the surfacial layer, limited by the permeation of light and diffusion of oxygen within polymers. Carbonyl index might not fully reflect the changes of surface alteration properties, as evidenced by the difference between carbonyl index and O/C. Therefore, XPS technique could be used as a supplemental tool to probe the surface alteration properties of microplastics. The O/C ratio can explain the oxygen-containing functional groups (e.g., C—O and O—H) that might not be included in the carbonyl index values, and high-resolution XPS spectra provided detailed information with respect to the polymer surfaces. Overall, the chemical alteration properties of microplastics could be evaluated more comprehensively based on both parameters of O/C ratio and carbonyl index.

To sum up, the above results indicated that aging behavior significantly alter the physicochemical properties of microplastics especially biodegradable PLA, inducing the surface physical deformation and chemical composition change. Actually, the natural weathering/aging of various microplastics is an extremely complicated processes accompanied with the heat, mechanical abrasion, aging of chemical substances (e.g., oxidizing agents, natural organic matters), UV radiation, biofilm attachment and biodegradation, and the leaching of additives. Consequently, the physicochemical properties of aged microplastics undergoing different environmental media and complicated aging approaches need to be comprehensively evaluated via diversified assessment indicators and a consensus criteria including physic and chemical aspects [23].

3.2. Adsorption kinetics of Pb(II) onto the representative microplastics

To estimate whether the metal ions leached from TWP caused the potential impact on the adsorption process, the release kinetics of typical metals within a week were initially investigated (Table S4). Results showed that Ca(II), total Cr, total Fe, Cd(II), Co(II), and total As were not leached from TWP, while the leaching concentration of Pb(II), Cu(II), Na (II), Mg(II), Ni(II) and Total Mn were detected at the 0 to several dozen μg/L level. Therein, the leaching concentrations of Pb(II) from TWP (mass: volume = 1 g/L) in the 2, 4 and 7 day were 1.16 ± 0.24, 0.36 ± 0.22 and 0 μg/L, respectively. Compared with the metal ion leached from the worn old tires (Table S2) and EDS analysis of TWP (Fig. 1C), these observations suggested that leaching contents of Pb(II) from TWP was negligible, so it might have little impact on the adsorption system. It is worth noting that the leaching amount of Zn(II) from Michelin worn tires was 631.13 ± 57.34 μg/L (Table S2), whereas Zn(II) leached from TWP in the 2, 4 and 7 day were 758.04 ± 15.91, 1088.99 ± 28.83 and

1137.00 ± 27.11 μg/L, respectively (Table S4). Similarly, a recent study demonstrated that the highest metal concentration at the mg/L level in the freshwater leachate from the arificial TWP (mass: volume = 80 g/L) was presence in Zn(II), and subsequently, the complex leachate significantly inhibited the growth and development of model aquatic organisms such as microalgae and mussels [27]. Due to the extensive and large amount of the TWP in the aquatic environment especially urban water systems, more attention should be paid to the distribution, fate and ecological risks of TWP itself or from their released chemicals (e.g., Zn (II), toxic organic compounds) [59,60]. Futhermore, a large amount of Zn(II) and complex organic compounds released from the inside of tire particles may affect the adsorption/desorption behavior of TWP in certain extent and need to further study in the future work. Likewise, a study reported that the leaching hexabromocyclododecane additives and related C-Br groups in the PS microplastics had a significant effect on Cd(II) adsorption [61].

The adsorption kinetics of Pb(II) onto five representative microplastics (UV-PLA, PLA, UV-PS, PS and TWP) were performed, and kinetic parameters fitted by the pseudo-first-order and pseudo-second-order adsorption models were noted in Table S6. The correlation coefficient (R^2) of the pseudo-first-order model and pseudo-second-order model was between 0.84-0.99 and 0.94–0.99, respectively. These results showed that the fitting degree of pseudo-second-order kinetics for Pb(II) adsorption was better than that of pseudo-first-order model kinetics. In addition, its calculated adsorption capacity was generally closer to the actual experimental adsorption values. Therefore, the pseudo-second-order kinetic model was more suitable for describing the adsorption process of five representative microplastics, suggesting that chemisorption might be the important factor limiting adsorption rate of metal ions onto microplastics [32].

The result of pseudo-second-order model was exhibited in the plots of adsorption kinetics (Fig. 4a), indicating the adsorption process of Pb (II) onto five kinds of microplastics from start to equilibrium. For UV-PS and PS, the majority of adsorption amounts were gained within 4 h and it gradually stabilized after 16 h. For UV-PLA and PLA, the vast majority of adsorption amounts were gained within 8 h, and the adsorption rate rapidly slows down as time goes by. After 24 h, their adsorption capacity nearly had no significant change, showing that these processes reached the adsorption equilibrium. Obviously, TWP showed a relatively slower adsorption process than that of the another four microplastics, its adsorption rate gradually slowed down until 24 h, and finally arrived the adsorption equilibrium at 36 h. From what discussed above, the adsorption rates among tire wear particles, biodegradable microplastics and conventional microplastics were significantly different, implying that the adsorption behaviors of heavy metals onto different composition of microplastics may continue through different adsorption

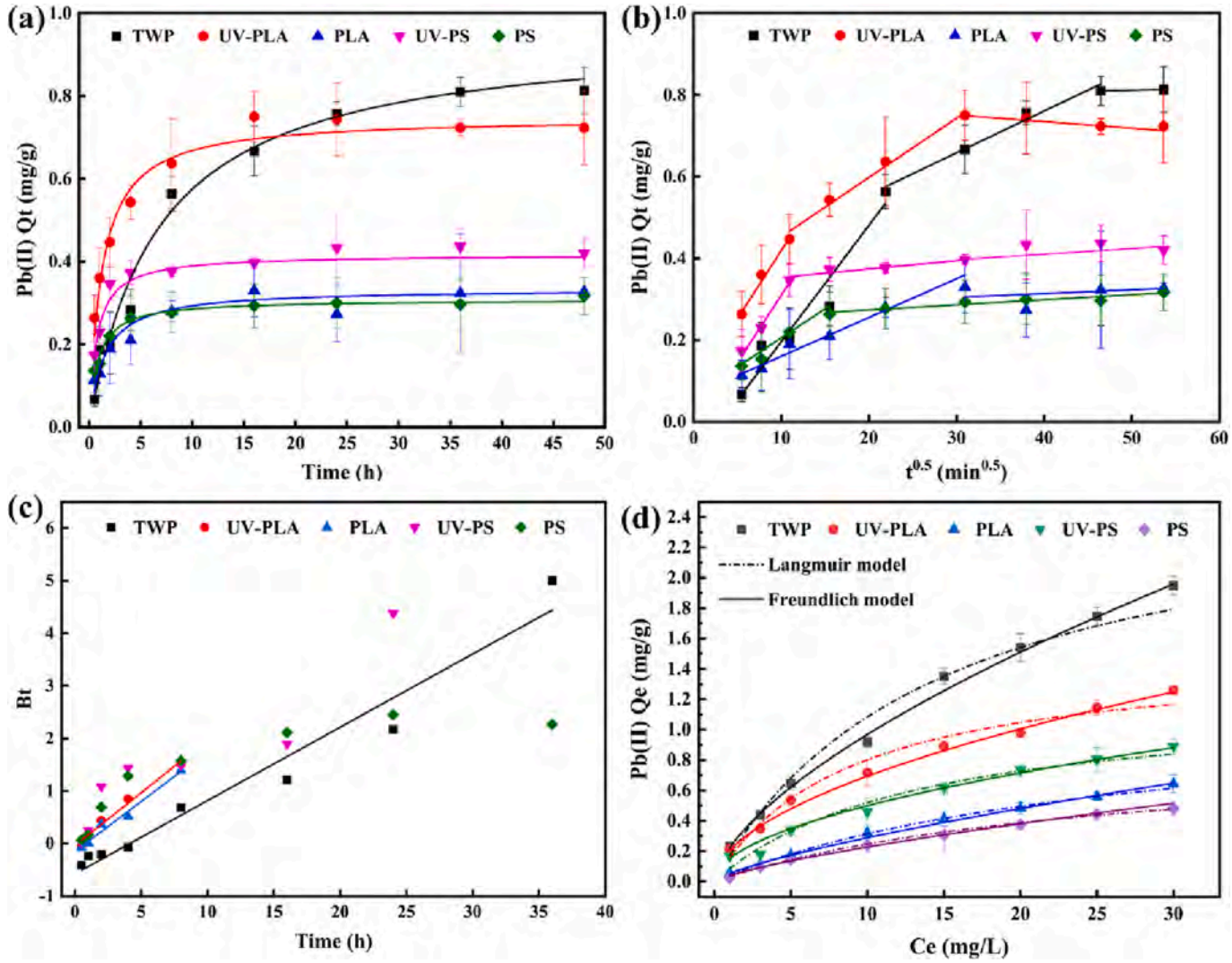

Fig. 4. (a) Adsorption kinetics of Pb(II) onto the TWP, UV-PLA, PLA, UV-PS and PS (Adsorption conditions: 10 mg/L Pb(II), solid/liquid ratio = 1 g/L, pH = 5.0 ± 0.1, 25 °C, reaction time 0.5–48 h); (b) Intraparticle diffusion plots for the adsorption of Pb(II) onto microplastics; (c) Film diffusion plots of Bt versus time (h); (d) Adsorption isotherms of Pb(II) onto microplastics (Adsorption conditions: 1–30 mg/L Pb(II), solid/liquid ratio = 1 g/L, pH = 5.0 ± 0.1, 25 °C, equilibrium time 48 h).

mechanisms.

The above two adsorption kinetics models could not explain the diffusion process of metal ions. In order to further understand the adsorption process of metal ions by the representative microplastics, the intraparticle diffusion model, which assumed ion adsorption affected by the complicated physicochemical process and occurred via a series of rate-limiting stage "Bulk transport - External film diffusion - Internal pore diffusion - Adsorption itself" [62], was adopted to fit the experimental adsorption data. The adsorption processes of Pb(II) onto the five representative microplastics fitted by intraparticle diffusion model were demostrated in Fig. 4b, and its fitting parameters were listed in Table S7. The fitting plots of five representative microplastics were respectively divided into two or three linear sections, indicating that there existed in different adsorption stages during the Pb(II) sorption process. The Pb(II) adsorption processes onto the TWP, UV-PLA and UV-PS were divided into three stages, while adsorption processes onto pristine PLA and PS were distributed in two stages. The initial linear section of Pb(II) symbolizes film diffusion and the subsequent linear sections represent intraparticle diffusion and quasi-equilibrium stage. Notably, the k_i value of aged microplastics (TWP, UV-PLA, UV-PS) in the first and second linear sections was distinctly greater than that of pristine microplastics (PLA, PS), implying a higher diffusion and adsorption rate onto aged microplastics. Meanwhile, the intercept c_i value became step-by-step greater, which explained the increase of boundary layer effects and progressive diffusion steps of metal ions. Furthermore, the two or three linear sections of all plots were away from the origin point, thus the rate-limiting stage of adsorption process might be not just affected by intraparticle diffusion. Generally speaking, the Pb(II) adsorption data fitted by intraparticle diffusion model showed the relatively high R^2 value in all linear sections, and the slope k_i value of all microplastics became the step-by-step smaller throughout linear sections, indicating that the diffusion rate of metal ion was getting lower and lower with an increasing internal diffusion resistance in pore, and finally adsorption process reached the quasi-equilibrium stage [63].

In addition, the Boyd plot of Bt versus time was used to further explain the rate-limiting stage and distinguish whether adsorption process of Pb(II) controlled by film diffusion or intra-particle diffusion. If a straight line in the plot went through the origin point, intra-particle diffusion was the rate-limiting stage, whereas the sorption process was governed by film diffusion [62,64]. As shown in Fig. 4c, the plots of Bt versus time in TWP, UV-PLA and PLA showed a significant linear relationship ($R^2 = 0.95$, 0.98 and 0.97, respectively), and the line was close to origin point but not passed through the origin point. This results implied that film diffusion was involved in the adsorption process and both intra-particle and film diffusion mechanisms were possibly existed [65]. For UV-PS and PS in Fig. 4c, film diffusion mainly governed the adsorption process. The aging behavior not only increase the diffusion and adsorption rate of metal pollutants onto aged microplastics, but also it and plastic types might affect the diffusion mechanism.

3.3. Adsorption isotherms of Pb(II) onto the representative microplastics

The adsorption isotherm plot of Pb(II) onto TWP, UV-PLA, PLA, UV-PS and PS was showed in Fig. 4d, and fitting parameters by Langmuir and Freundlich model were recorded in Table S8. According to the R^2 values, the adsorption isotherms of microplastics were better fitted by Freundlich model (0.981–0.998) than by Langmuir model (0.910–0.995) except PS microplastics, indicating that adsorption processes were performed on a heterogeneous surface due to the pore, crack and rough surface after aging/weathering [43]. Furthermore, the interaction of TWP, UV-PLA, PLA and UV-PS with Pb(II) can be considered as a multi-layer adsorption attributed to the adsorption site heterogeneity, while the adsorption onto PS may occurr as a monolayer adsorption. In the Freundlich model, the K_F values of five representative microplastics were followed the order of TWP > UV-PLA > UV-PS > PLA > PS, suggesting the maximum adsorption ability of TWP to Pb(II). As for Langmuir model, the adsorption isotherm of TWP showed the largest adsorption capacity (q_m) compared with the other four types of microplastics. TWP had the Pb(II) adsorption amounts with a theoretical value of 2.665 mg/g, followed the order by UV-PLA (1.509 mg/g), UV-PS (1.210 mg/g), PLA (1.173 mg/g) and PS (0.894 mg/g). These results implied a distinct enhancement to the adsorption of metal ion onto all types of microplastics after the aging/weathering processes because aging behavior can lead to the surface heterogeneity of polymer and growth of adsorption sites.

The comparison of adsorption ability and mechanism of different aged microplastics to metal ions onto was listed in Table S10. Broadly speaking, the different types of aging/weathering behavior, such as naturally-exposed aging, UV radiation, mechanical abrasion, chemical oxidant aging, biofilm attachment and biodegradation, significantly increased the adsorption capacity of aged conventional microplastics (e.g., PE, PP, PVC, PET, PMMA, PP, PA, PS) to metal ions (e.g., Pb(II), Cd (II), Cu(II), Co(II), Cr(VI), Ni(II), Zn(II), Ag(I), As(III), Hg(II)), than the pristine conventional microplastics. Our results implied that the aging process obviously promoted the adsorption capacity of all types of microplastics, and the environmentally-relevant TWP had the greater adsorption ability to Pb(II) than the aged biodegradable microplastics, eventually follwed by the conventional microplastics. Similarly, Sun et al. [66] reported that the biofilm-attached PLA showed the higher monolayer Cu(II) adsorption capacity of 1045.67 ug/g than that of pristine PLA (151.802 ug/g), which was attributed to the surface complexation between Cu(II) and functional groups contained in biofilms. Moreover, the aged TWP had the greater adsorption ability than the aged conventional microplastics to toxic metal ions and organic contaminants [28,29,67]. In short, the environmentally-relevant TWP and aged biodegradable microplastics can be served as actually stronger "vectors" of environmental pollutants than the conventional microplastics, thus it is urgent to further clarify their adsorption mechanisms and underlying ecological risks.

3.4. Adsorption mechanisms

In our evaluation results, UV-PLA and UV-PS had the irregular and rougher surface structure with a series of cracks, pits and bumps, and the more peeling layers and smaller broken particles were formed on the surface of UV-PLA (Fig. 1 and Fig. S3). As shown in the Table 1, the specific surface area (15.37–3.84 m^2/g) and pore volume (0.012–0.0029 cm^3/g) of pristine/aged microplastics were followed the order by UV-PLA > UV-PS > PLA > PS and brought into correspondence with the orders of the maximum adsorption capacities of these microplastics to Pb(II). Another reason for UV-PLA with the greatest adsorption capacity can be attributed to its smallest particle size due to the fragmentation and destroy of photo-oxidation/degradation (Fig. S3 and Table 1). According to the previous studies, the crystallinity of microplastics was likely to a nonnegligible factor affecting the adsorption of environmental pollutants such as metal ions and organic pollutants onto the pristine microplastics [68]. In this study, UV-PLA had the highest crystallinity of 16.52 ± 1.04 % and the second adsorption capacity, whereas TWP with the greatest adsorption ability had a relatively smaller crystallinity (2.50 ± 0.12 %) than that of PLA (3.93 ± 0.54 %) (Table 1). For UV-PS and PS, its crystallinity was too poor to be calculated. Broadly speaking, the crystallinity of the five microplastics was not incompletely consistent with the order of adsorption capacity. Compared with that before adsorption of microplastics (Fig. 2d), Fig. 5a showed that the formation of a new crystalline phase between 20 and 25° arised in the TWP, UV-PS and PS after the adsorption of Pb(II), while the crystallization peak of UV-PLA and PLA was strengthened at the similar locations. Overall, these results suggested that crystallinity affect the adsorption of pristine/aged microplastics, but it might be not the dominant factor influencing the adsorption mechanism of metal pollutants.

In addition, UV aging significantly reduced the Zeta potential on the

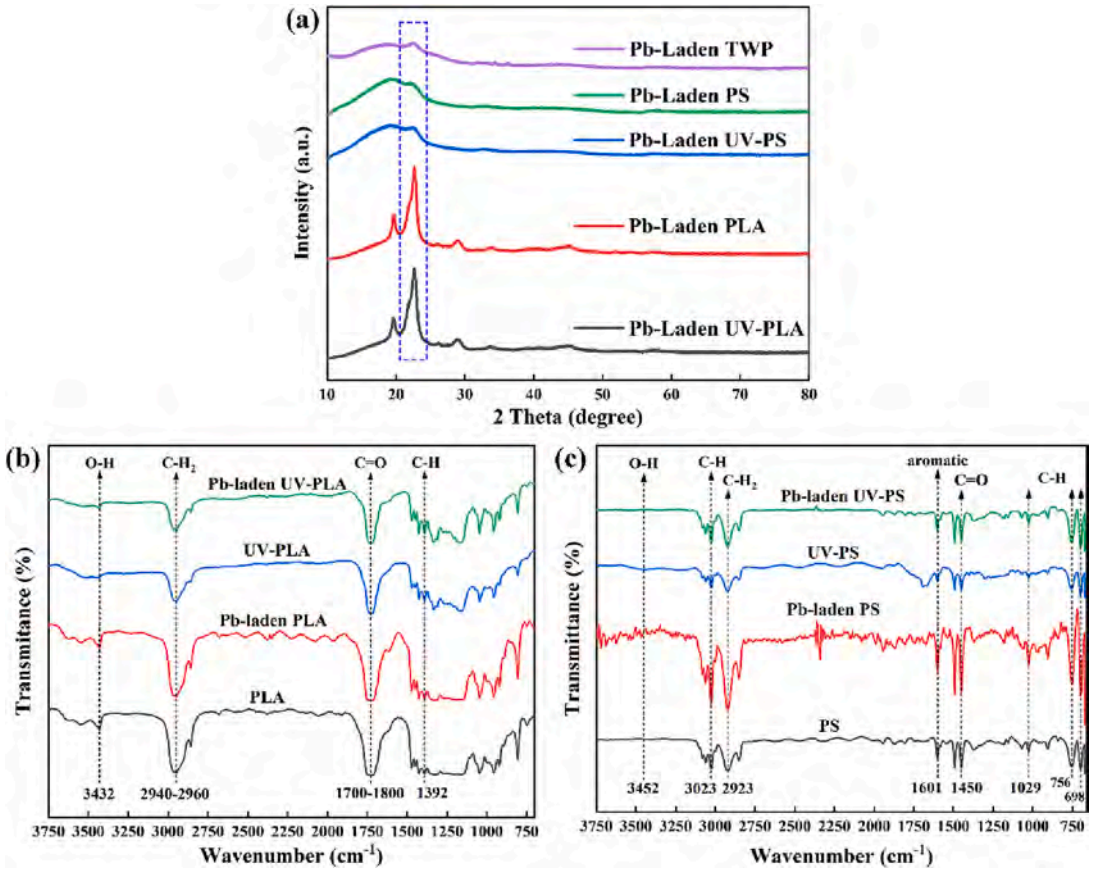

Fig. 5. (a) XRD spectra of UV-PLA, PLA, UV-PS, PS and TWP after adsorption of Pb(II); FT-IR spectra of the (b) PLA and UV-PLA, and (c) PS and UV-PS before and after adsorption of Pb(II).

microplastics under the solution pH range from 2 to 7, and the magnitude of values was followed the order: UV-PLA < UV-PS < PLA < PS (Fig. 2c), which was in accordance with the order of maximum adsorption capacities of four microplastics at the aqueous pH of 5. This fact can explain the greater adsorption capacity of Pb(II) on aged microplastics than pristine microplastics probably due to the more negative charged surface. Following, Fig. 9a showed that adsorption capacity of UV-PLA to Pb(II) under any same solution pH ranged from 4 to 7 was larger than that of UV-PS with a larger Zetal potential, further revealing the the significant function of electrostatic interaction in the adsorption of metal pollutants onto the biodegradable and conventional microplastics.

The surface functional group species of four representative microplastics including UV-PLA, PLA, UV-PS and PS before and after the adsorption of Pb(II) was displayed in the FT-IR spectra (Fig. 5). Theoretically, the adsorption ability of microplasitcs was markedly dependent upon the chemical structure of the plastic polymer itself and their potential interactions with environmental pollutants [33,69]. Herein, the spectra shapes of four microplastics were similar before and after adsorption of Pb(II), and the primary adsorption peaks roughly appeared in similar positions. Notably, the obvious enhancement in peak areas and peak intensity of functional groups, including the C═O and aromatic groups in UV-PS and PS after adsorption and C═O and O—H in UV-PLA and PLA, were observed in Fig. 5(b-c). As can be seen from the evaluation results of chemical properties of aged microplastics (Fig. 3c, Table 1), the carbonyl index and O/C ratio of PLA and PS were increased to varying degree after the aging process, suggesting the significant enhancement of oxygen-containing functional groups. These increasing contents of oxygen-containing functional groups were closely related to the greater adsorption capacity of metal ions onto the aged microplastics [49]. Therefore, above results manifested that the oxygen-containing functional groups play an important part in the metal adsorption mechanism onto the aged biodegradable and conventional microplastics. In addition, the significantly increased intensity of aromatic groups (1601 cm^{-1}) in the conventional microplastics UV-PS and PS after Pb(II) adsorption indicated the certain interaction occurred between the benzene ring structure of microplastics and Pb(II), and meanwhile, the obvious variation of aromatic C—H out-of-plane bending at 675–1050 cm^{-1} (e.g., 698, 756, 1029 cm^{-1}) was observed after the Pb(II) adsorption (Fig. 5c). These phenomenons implied that the cation-π interaction might be involved in the Pb(II) adsorption process [70].

Although TWP showed the serious rough and fluffy surface structure and strongest adsorption capacity than that of UV-PLA, UV-PS, PLA and PS, it did not exhibit the excellent physical properties (e.g., specific surface area, pore volume, particle size, Zeta potential) conducive to adsorption (Fig. 1, Fig. 2, Table 1). For example, TWP had the minimum specific surface area and total pore volume than the other four pristine/aged microplastics, otherwise its particle diameter distribution was the largest. Besides, it had the greatest adsorption ability to Pb(II), but its Zeta potential was higher than US-PLA and UV-PS, suggesting that electrostatic interaction was likely to not the dominated adsorption mechanism for TWP (Fig. 2c and Fig. 9a). In this study, the O-PTIR was applied to visualize and analyze the TWP samples (Fig. 6). As expected, this advanced technique examined the IR absorption signals from the submicrometre-resolved TWP surface and revealed its chemical properties before and after the Pb(II) adsorption process. The O-PTIR spectra of Pb-laden TWP (sampling positions number 9–12) showed some differences with the sampling positions (number 1–8) of TWP before Pb(II) adsorption (Fig. 6a and b). The 1500–800 cm^{-1} wavenumbers were mainly composed of the absorbance bands of elastomer components, filler SiO_2 and carbon black [71]. The broad absorption band from 1000

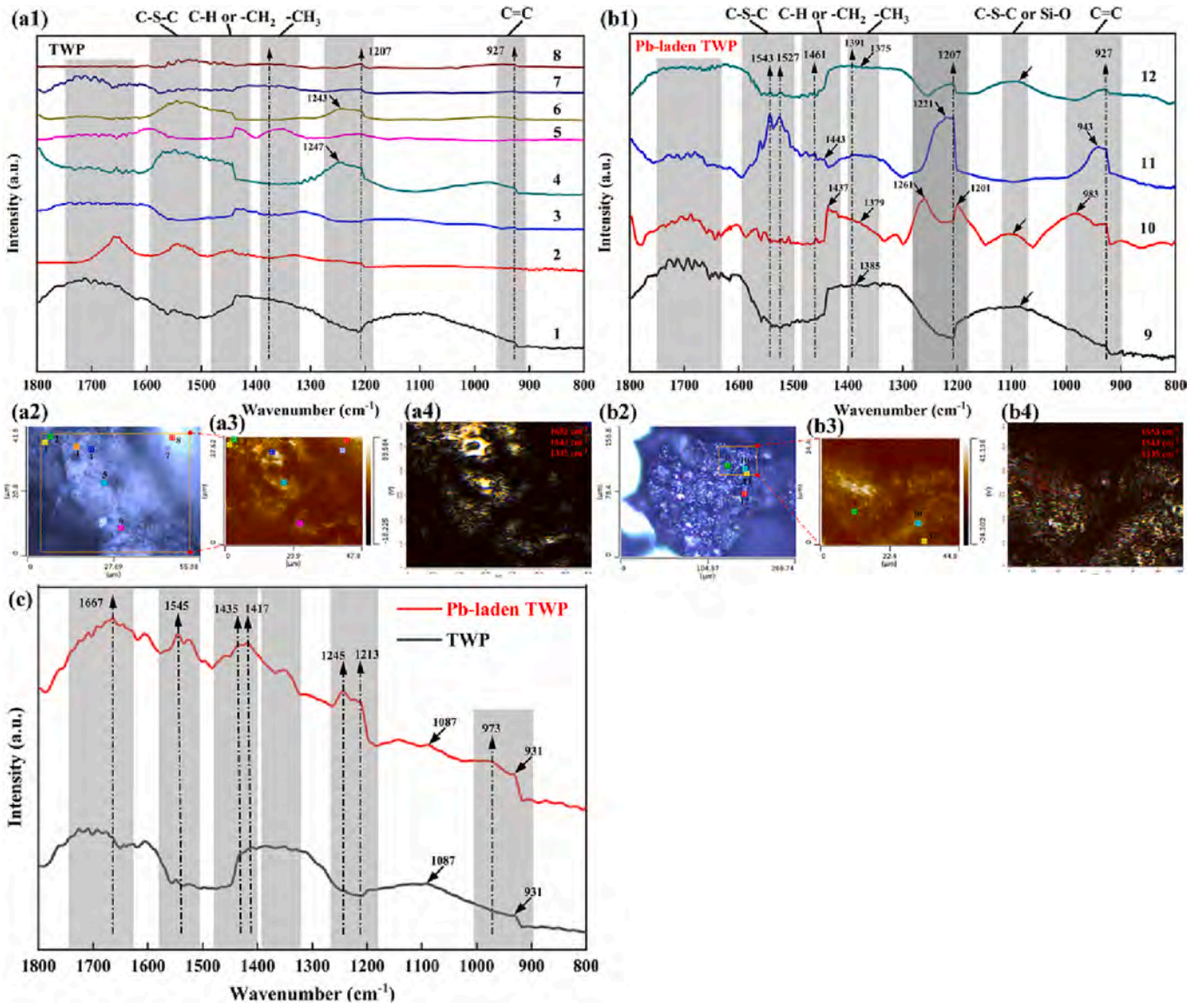

Fig. 6. High-resolution O-PTIR analysis of TWP (a1-a4) before and (b1-b4) after adsorption of Pb(II) in the sampling area. Note: (a1) and (b1) mean O-PTIR spectra of sampling positions number 1–12 in TWP; (a2) and (b2) exhibited the optical images in the sampling area of TWP samples; (a3) and (b3) showed the imaging of IR laser beams focused on TWP surface through a reflective objective; (a4) and (b4) revealed the overlay mapping maps at three representative IR beams (1335, 1543, 1653 cm^{-1}) determined for the sampling area of TWP surface. (c) Overall comparison of the averaged O-PTIR spectrum of spectra in TWP sampling positions before and after Pb(II) adsorption. Visible-laser and O-PTIR images were sample-dependently acquired at a high-resolution of 50–500 nm per point, a rate of 10–1000 μm s^{-1}, a visible-laser power of 5 or 9 %, an IR power of 8 or 17 % and a detector gain of 2 × or 5 ×. The O-PTIR spectra were normalized and the overlay mapping maps or average O-PTIR spectra of TWP samples were processed and gained by PTIR Studio software (Photothermal Spectroscopy Co., ltd).

to 900 cm^{-1} (927, 943, 983 cm^{-1} in Fig. 6b) was attributed to C═C stretching [72]. The IR absorption bands at 1100–1070 cm^{-1} probably contained C—S—C groups [72,73] and/or Si-O stretching [71]. In addition, the band at 1400–1370 cm^{-1} (1375, 1379, 1385, 1391 cm^{-1} in Fig. 6b) may be linked to the presence of $–CH_3$ groups [71,74]. On the basis of the IR absorption at 1480–1430 cm^{-1} (1437, 1443, 1461 cm^{-1} in Fig. 6b), the TWP particles might included C—H and/or $–CH_2$ groups [71,73,74]. The overlapping bands from 1590 to 1500 might be associated to the C—S—C groups, which are usually linked to the vulcanization reaction of rubber [75]. Moreover, a overlapping band in 1750–1600 cm^{-1} and a broad band in 1260–1200 cm^{-1} (1201, 1207, 1221, 1261 cm^{-1}) were showed in the O-PTIR spectrum of TWP before and after adsorption of Pb(II). Notably, the averaged O-PTIR spectrum of spectra in sampling positions of TWP (number 1–8) and Pb-laden TWP (number 9–12) was compared in Fig. 6c. The IR absorption bands of Pb-laden TWP clearly distinct from that of the TWP without adsorption of Pb(II). These results indicated that the C band and some functional groups (e.g., C═C, Si-O, C—S—C) were highly likely to play critical roles in the process of metals adsorbing onto TWP particles. Furthermore, the properties of complex carbon-based mixtures (e.g., synthetic and/or natural rubbers, carbon black and additive polymers) in TWP were closely linked to its excellent adsorption ability beyond than other aged microplastics.

The XPS spectra was used for further revealing the variation of surface properties on the five representative microplastics including TWP, UV-PLA, UV-PS, PLA and PS. The main elements (C, O) and their peaks of C 1 s and O 1 s were detected in the XPS survey spectra of all microplastics before and after Pb(II) adsorption. The new slight peaks of Pb 4f were found in the TWP both before and after adsorption and UV-PLA and UV-PS after adsorption (Fig. S5), which suggested that Pb(II) was successfully adsorbed on the surface of aged microplastics. Moreover, the proportions of C and O on all microplastics surface was

changed after adsorption. The peaks of C 1 s spectra of all microplastics both before and after adsorption of Pb(II) were shown in Fig. 7. Notably, the variation trend of C═C/C—C, C—H, C—O, C═O and O-C═O before and after Pb(II) adsorption varied from the types of microplastics. For the TWP in Fig. 7a, the C 1 s spectra of TWP before Pb(II) adsorption was deconvoluted into two peaks at 284.80 and 285.05 eV, probably corresponding to C—C and/or C═C bonds, and C—S, C—O and/or C═O bond respectively. The content of functional groups including C—S, C—O and C═O, with a limited amount, was enhanced after Pb(II) adsorption, and its peak of the binding energy from 285.05 eV was shifted to 285.16 eV. In addition, the new peak at 288.36 eV corresponded to O-C═O band. These transformations illustrated that the adsorbed Pb(II) might lead to complexation reactions in the complex rubber co-polymer and result in these change of the functional groups. As exhibited in Fig. 7b, The C1s spectra of UV-PLA can be separated into four sub-peaks including C—C, C—O, C—O—C and O-C═O/C═O, and their their banding energy were 284.80, 286.13, 287.10 and 288.68 eV, respectively. Compared with the pristine PLA, the contents of C—C and C—O—C groups in UV-PLA decreased while the content of C—O, O-C═O and/or C═O increased, and positions of banding energy in C—O—C groups was obviously shifted from 286.75 to 286.94 eV, indicating the the chemical oxidation of main chain and enhancement of oxygen-containing groups during the aging process. After the Pb(II) adsorption onto PLA and UV-PLA, the varying degrees of increase of C—O, C═O and/or O-C═O groups, and decrease of C—O—C contents and its significant shift in binding energy, further verified the significant effect of oxygen-containing functional groups during the adsorption process (Fig. 7b and 7c). As shown in Fig. 7e, the C 1 s spectra of PS could be deconvoluted into three individual peaks, corresponding to aromatic C—H, aliphatic C—H, and π-π* shakeup (the characteristic component of

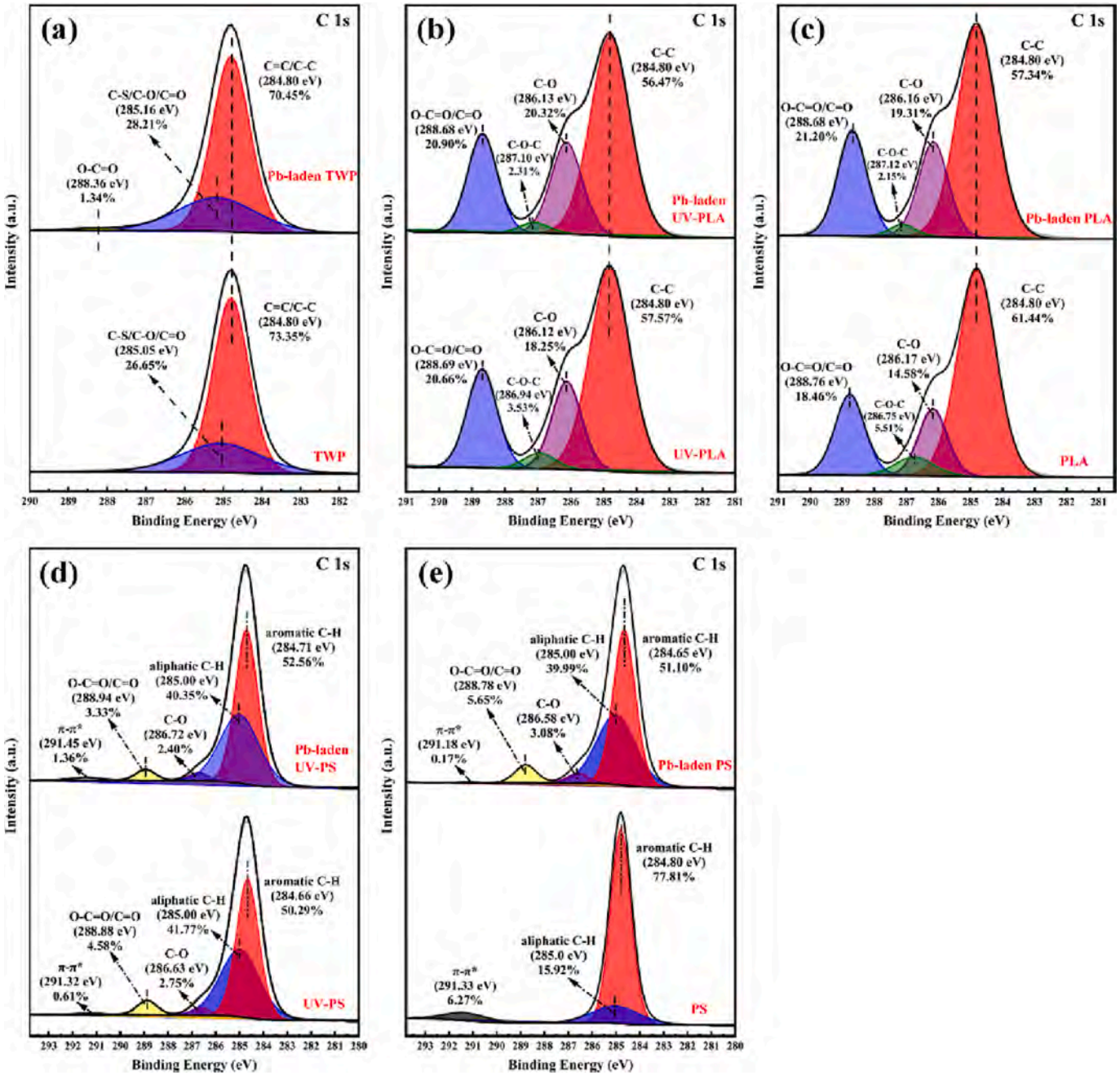

Fig. 7. XPS C 1 s spectra analysis of (a) TWP, (b) UV-PLA, (c) PLA, (d) UV-PS, and (e) PS before and after adsorption of Pb(II).

phenyl rings) at 284.80, 285.0 and 291.33 eV, respectively. After the aging process, the intensity of π-π* in UV-PS was markedly decreased from 6.27 % to 0.61 % (Fig. 7d), and concurrently, the relative proportion of aromatic C—H decreased and aliphatic C—H increased, which might be attributed to the opening of benzene rings or the volatilization of small molecules containing benzene rings from the PS backbone [58]. It could be observed that, after the adsorption of Pb(II) onto PS, the emerging peak at 286.58 and 288.78 eV binding energy corresponded to C—O and O-C═O/C═O, respectively, suggesting the significant role of complexation of oxygen-containing functional groups in the adsorption. For the UV-PS in Fig. 7d, the π-π* peak at 291.32 eV was increased from 0.61 % to 1.36 % at 291.45 eV after the Pb(II) adsorption and aromatic C—H at 284.66 eV was also promoted from 50.29 % to 52.56 % at 284.71 eV, while the contents of oxygen-containing groups was reduced. These variation indicated the certain alteration of aromatic structure after the Pb(II) adsorption, and thus, the cation-π interaction probably involved the adsorption process of UV-PS. On the other hand, the variation of proportion in peaks of O 1 s spectra of all microplastics after adsorption of Pb(II) and related shift of position of binding energy in some peaks confirmed that oxygen-containing functional groups especially C—O, C═O and O-C═O were very important for the adsorption of Pb(II) onto aged microplastics (Fig. S6). In addition to the relatively excellent physical structure (e.g., the rougher surface, larger specific surface area and pore volume, smaller particle size and more negative Zeta potential) than the pristine microplastics, the above findings revealed that the electrostatic interaction, complexation of oxygen-containing functional groups and cation-π interaction involved the crucial contribution in the process of metal adsorption onto aged microplastics, whereas there were some differences in adsorption mechanisms among different aged microplastics (Fig. 8).

3.5. Effects of aquatic chemistry on Pb(II) adsorption processes of aged microplastics

3.5.1. The effect of pH

The solution pH can alter the surface charge of materials and speciation of heavy metal ions, thus it was generally regarded as an important factor affecting the adsorption capacity and properties of microplastics in the aquatic surroudings. The effect of pH on the Pb(II) adsorption capacity of aged microplastics was exhibited in Fig. 9a, showing that the adsorption capacity of all aged microplastics were increasing with the increasing pH value from 4 to 7, while the Zeta potentials of these aged microplastics steadily decreased. When pH > pH_{pzc}, the increasing adsorption capacity was mainly due to the increase of microplastic surface anions in the aqueous pH range, explaining the significant effect of electrostatic interaction in the adsorption of aged microplastics to Pb(II) [76]. Notably, the adsorption amounts of aged microplastics was followed the order of TWP, UV-PLA and UV-PS in the whole solution pH values (4–7), whereas the magnitude of Zeta potential was in order of TWP, UV-PS and UV-PLA, respectively. Thus, the weakest surface electronegativity with the strongest adsorption ability indicated that electrostatic interaction was not the most effective mechanism determining the adsorption capacity of TWP. Besides, the maximum adsorption capacity was observed for Pb(II) at pH = 7, which may be attributed to the formation of hydroxides such as $PbOH^+$, $Pb(OH)_2$, and $Pb_3(OH)_4^{+2}$ [77]. In brief, the electrostatic interaction played an important role in the adsorption of heavy metal ions onto aged microplastics.

3.5.2. The effect of HA

As shown in Fig. 9b, the low concentration of HA enhanced adsorption capacity of Pb(II) onto three types of aged microplastics, otherwise the high concentration of HA inhibited it. In the range of 1–10

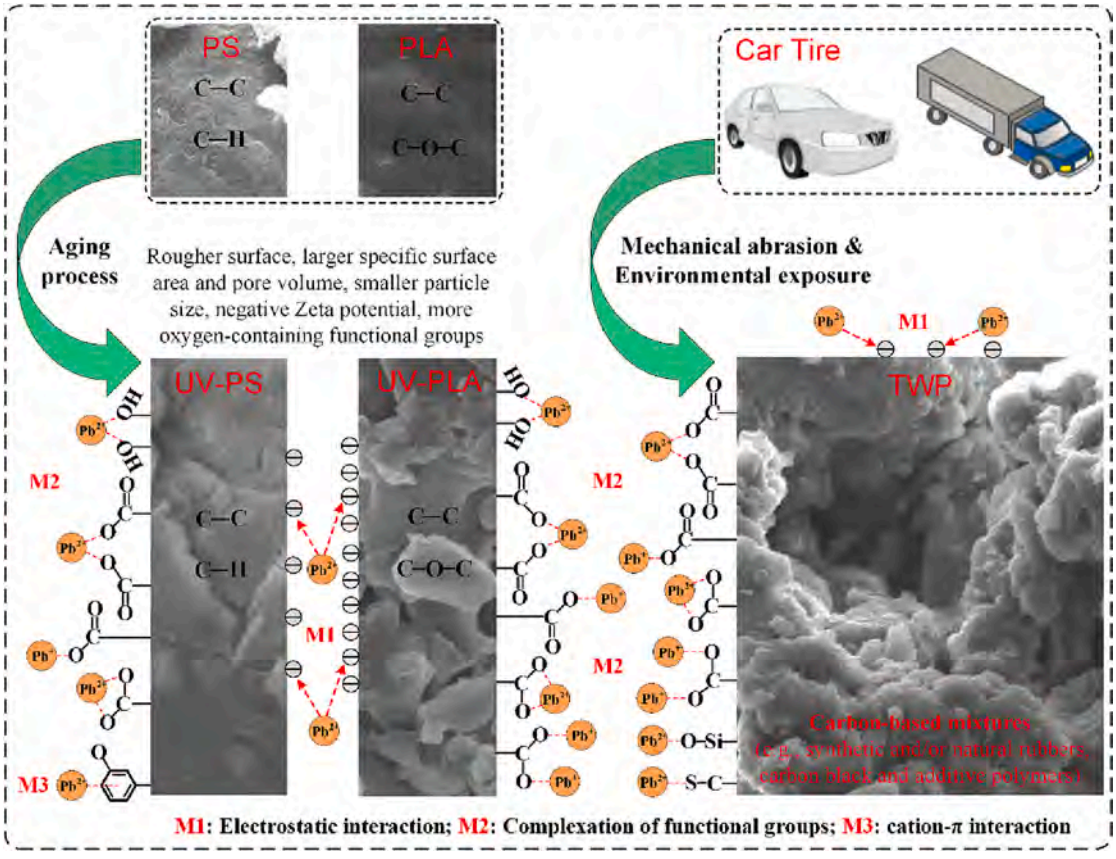

Fig. 8. Adsorption mechanisms of Pb(II) on aged microplastics (UV-PLA, UV-PS and TWP).

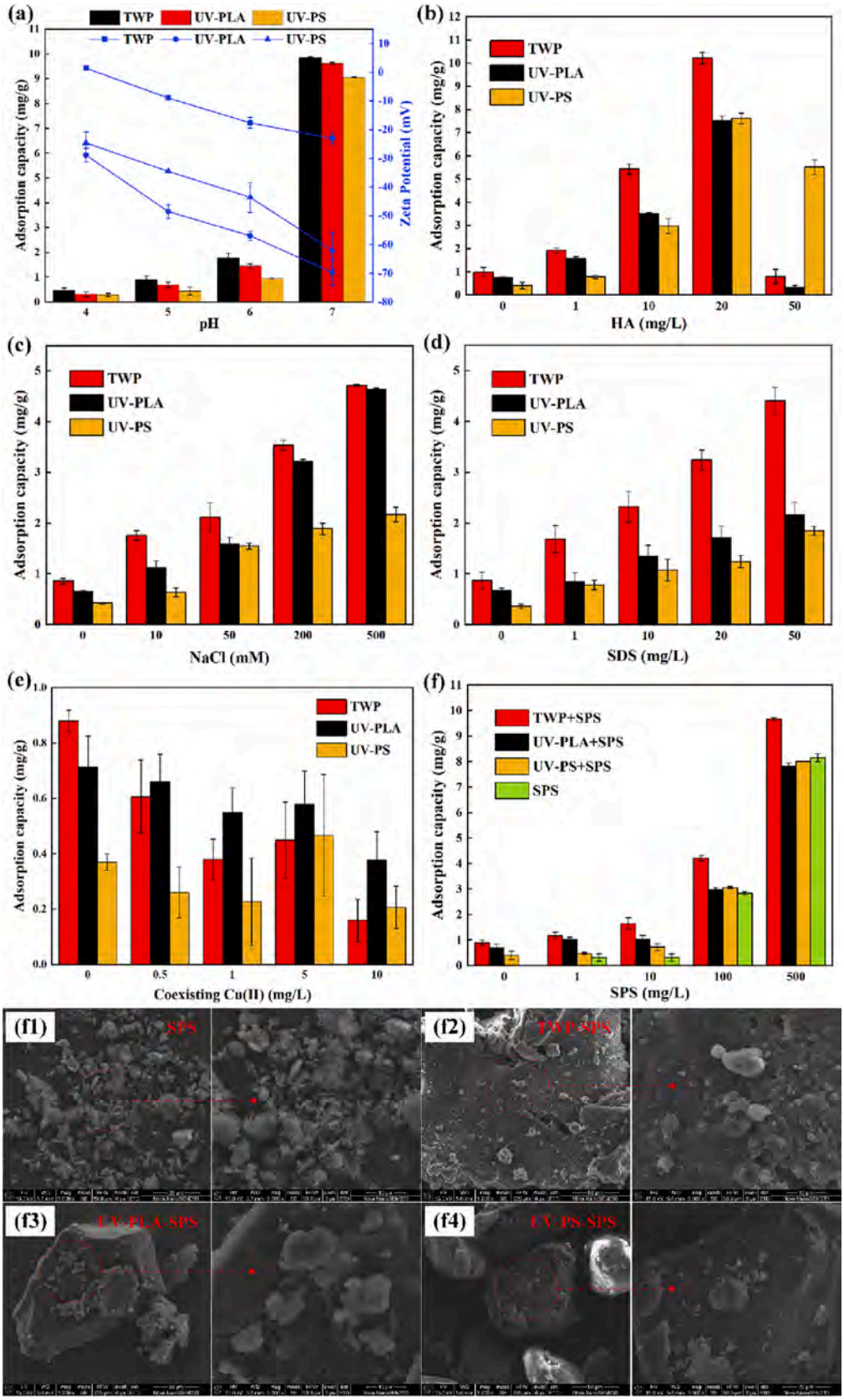

Fig. 9. Effect of (a) pH (4–7), (b) humic acid (HA, 0–50 mg/L), (c) salinity (NaCl, 0–500 mM), (d) surfactant SDS (0–50 mg/L), (e) coexisting Cu(II) (0–10 mg/L) and (f) suspended sediment (SPS, 0–500 mg/L) on the adsorption of Pb(II) (10 mg/L) onto aged microplastics (TWP, UV-PLA and UV-PS, 20 mg per 20 mL Pb(II)); (f1-f4) SEM images of the complexes of Microplastics-SPS.

mg/L HA, the adsorption capacity of the three types of aged microplastics for Pb(II) increased quickly, and the order of adsorption capacity was TWP, UV-PLA, UV-PS, respectively. Notably, there are some interesting phenomenons in the adsorption performance by the different aged microplastics in the presence of high dose of HA. When the concentration of HA reached 20 mg/L, the adsorption capacity of all aged miroplastics for Pb(II) rapidly achieved the maximum values and that of TWP was the largest among them, but the adsorption capacity of UV-PS was slightly higher than that of UV-PLA. Then, the adsorption ability of UV-PLA and TWP to Pb(II) sharply declined at the highest concentration of HA (50 mg/L), while the final order of adsorption capacity was UV-PS > TWP > UV-PLA. Compared with TWP and UV-PLA, the adsorption of UV-PS was significantly less affected by the high concentration of HA.

Generally speaking, our results implied that organic matter molecules in the aquatic environment played a dual role in the adsorption behavior of aged microplastics to Pb(II). When the HA concentration is low in the aquatic environment, HA can occupy a part of adsorption sites in the surface of miroplastics and form a conjugated co-polymer, resulting in the increasing contact angle, more negative Zeta potential and stronger electrostatic interaction [78,79]. Thus, the adsorption capacity of Pb(II) onto UV-PLA, UV-PS and TWP was prominently promoted with the increasing concentration of HA. The similar enhancement phenomenon was showed in the adsorption of Cd(II) onto PS and PVC microplastics as co-existed in the 0–80 mg/L of humic substances [80]. As the concentration of HA got higher and higher, its absorbed amounts onto microplastics significantly increased and occupied the adsorption active sites because of the complex mechanisms including functional groups, hydrogen bond, hydrophobicity, electrostatic binding and n-π electron donor–acceptor [81]. This intensifying binding behavior reduced the direct contact between aged microplastics and Pb(II). Moreover, a large amount of free negatively-charged HA molecules can offer new adsorption sites, directly causing the complexation interaction between HA and Pb(II) and generating the competitive adsorption with aged microplastics in the aquatic surrouding. Furthermore, HA-Pb(II) coordination complexes in the solution might affect the Pb(II) adsorption onto aged microplastics. Therefore, the mechanism for suppression of natural organic matter to Pb(II) adsorption onto UV-PLA, UV-PS and TWP was explained by the above-mentioned dual competitive effects of HA at the high concentration. This finding is similar with the reported results of Tang et al. [51], they demonstrated that a preferential complexation between fulvic acid and Pb(II) resulted in the reduced Pb(II) adsorption onto the naturally-aged nylon microplastics with the increase of FA concentration. As for the smaller adverse effects of Pb(II) adsorption onto UV-PS, this may be due to the smaller number of functional groups and relatively weak electrostatic interaction on the surface of UV-PS and then HA did not occupy all adsorption sites of Pb(II), so UV-PS still maintained a relatively high adsorption capacity with the increasing concentration of HA. In natural environments, microplastics can be interacted with natural organic matters with a relatively low concentration, and their complexes showed the excellent adsorption capacity and altered fate and ecotoxicity of microplastics and metals.

3.5.3. The effect of salinity

Fig. 9c displayed that the adsorption capacity of Pb(II) onto the three types of aged microplastics (UV-PLA, UV-PS and TWP) gradually increased in all ranges of NaCl (0–500 mM). The adsorption capacity of TWP was higher in any NaCl concentration, and order of adsorption amounts to Pb(II) was TWP, UV-PLA and UV-PS, respectively. It is noteworthy that with the increase of NaCl concentration, the adsorption capacity of UV-PLA for Pb(II) gradually approached that of TWP, while the enhancement to Pb(II) adsorption onto UV-PS was relatively small. It might be explained by the fact that the presence of salinity could compress the electrical double layer at the adsorbent surface and led to the formation of plastic cluster, resulting in the stronger electrostatic interaction to pollutants than the single particulates and thus increasing the adsorption capacity [43]. Nevertheless, Tang et al. [51] found that salinity (NaCl, 0–3.5 %) significantly inhibited the absorption of Pb(II) by naturally-aged nylon microplastics, which was attributed to the increasing monovalent cations (Na^+) competitive adsorption, reduced electrostatic attraction and coulombic energy, and compressed electrical double layer effects. To summarize, Na^+ have both positive and negative impacts on adsorption behavior of microplastics to pollutants, thus further exploration is needed to elucidate the potential mechanisms for these different phenomenons about the impacts of salinity on microplastic adsorption.

3.5.4. The effect of surfactant

Due to the great demand in the domestic and industrial applications, various chemical surfactants, as a typical emerging contaminant existed in the wastewater with the high concentration at mg/L level, can be intentionally or unintentionally discharged into natural water bodies especially urban water systems [82]. Surfactants can be adhered to microplastic surface, decrease the interfacial tensions between liquid and solid, and enhanced the dispersion of pristine microplastics (e.g., PE, PP, PS, PMMA) to form a stable suspension, affecting the migration of different microplastics in the environmental media [44,83]. As shown in Fig. 9d, sodium dodecyl sulfate (SDS), one of the most widely used anionic surfactant in domestic and industrial aspects, significantly promoted the Pb(II) adsorption on aged microplastics within the concentration range of 0–50 mg/L. The order of adsorption capacity to Pb(II) was TWP, UV-PLA and UV-PS, respectively.

This promoting adsorption phenomenon can be explained by the presence of critical micelle concentrations (CMC) of surfactants. The ambient concentration (0–50 mg/L) of SDS surfactant used in this experiment was much lower than its CMC concentration (0.0086 M) [84]. Herein, a large amount of free-state SDBS with the increasing concentration increased the dispersion degree of UV-PLA, UV-PS and TWP, and further enhanced interfacial interaction between aged microplastics and Pb(II) in the solution. Moreover, a part of SDS molecules can be absorbed and adhered onto the rough surface of aged microplastics especially TWP and UV-PLA and might increase their electrostatic interaction, potentially leading to the increasing adsorption capacity to metal ions. Similar, Zhang et al. [85] reported that anionic surfactant sodium dodecyl benzenesulfonate (SDBS) at the concentration of 0–4 mM had a three-step effects (“increase-kept constant-decrease”) on the adsorption of Cr(VI) by pristine PE beads (177–250 μm), which were attributed to the the dual effects of the CMC concentration for SDBS. In fact, the concentration of surfactants existed in the natural waters are far lower than their CMC concentration that usually keep up to a few hundred mg/L [82]. Thus, surfactants can interact with microplastics in the environmental media, affect their migration behavior and significantly increase the “vector” effect to environmental pollutants, posing a nonnegligible hybrid environmental hazards.

3.5.5. The effect of Cu(II) coexistence

Previous studies have showed that Cu(II) can be absorbed by aged microplastics, and adsorption process may occur on the same adsorption sites of microplastics as Pb(II). As exhibited in Fig. 9e, within the range of 0–10 mg/L co-existing Cu(II), the adsorption capacity of UV-PLA, UV-PS and TWP to Pb(II) generally decreased with the increase of the concentration of co-existing Cu(II). The adsorption ability of TWP significantly suppressed by Cu(II), otherwise UV-PLA and UV-PS were less disturbed and even the adsorption capacity of UV-PLA was greater than that of TWP after the addition of Cu(II). Notably, a temporary increase in the adsorption ability to Pb(II) was appeared at the 5 mg/L Cu (II), but then it decreased to the minimum adsorption capacity. In general, the coexisting Cu(II) ions inhibited the adsorption capacity of Pb(II) onto the aged microplastics, mainly because adsorption process of Pb(II) and Cu(II) occurred in common adsorption binding sites of the surface of aged microplastics and resulted in the competitive adsorption to some extent. As showed in a previous study by Huang et al. [86], the

increasing concentration of several mixed metal ions solution (e.g., Cu (II), Pb(II), Zn(II), Mn(II)) significantly reduced the adsorption rates onto the aged LDPE pellets because of the fewer co-available adsorption sites, and the addition of iron ions changed the surface loading amounts of these metals onto microplastics surface due to the different affinity of metal ions to the plastic surface. Moreover, the adsorption capacity of pristine, UV-aged and biofilm-attached PS to Pb(II) or Cu(II) was all suppressed with the increasing concentration of interfering metal at the concentration of 0.005–0.1 mmol/L in the binary system of Cu(II) and Pb(II) [76]. To sum up, thefinding revealed that the coexistence of multiple contaminants can affect the metal adsorption amounts onto aged microplastics to different degrees and their discrepant distribution mechanisms on plastic surface are required to elucidate.

3.5.6. The effect of SPS

Suspended sediments (SPS), an ubiquitous and extremely important media in different aquatic environments especially river systems, are generally consist of inorganic particles, organic matter and microbial community [52]. In the last few years, the comparison of adsorption behavior and ability to metal ions between SPS and microplastics has been investigated. Besson et al. [87] found that 2.5 % of Cd(II), 68.0 % of Cs(I), and 71.0 % of Zn(II) in the seawater with a nominal metal concentration of 10 kBq/L were adsorbed in sediment particle, while pristine PE microplastics only adsorbed <0.8 % of these three metal ion, suggesting an insignificant vector effect of pristine microplastics. Although natural substrates (e.g., SPS, surficial sediments, algae particles) had a greater adsorption capacity to different metal ions, the naturally-aging significantly improved the adsorption amounts of aged conventional microplastics (e.g., biofim-attached PS and PE) and even made it nearly reaching to the level of natural substrates [32,34]. Generally, the adsorption capacity of aged conventional microplastics can be gradually enhanced with the increasing environmental aging/wearthing time [49,55,88]. Moreover, the pristine PS nanoplastics or PE microplastics can interact with SPS and form heteroaggregates [45]. However, the effect of interactions between aged microplastics and SPS on the adsorption of metal ions remains unknown.

The basic physicochemical properties of SPS were listed in Table S3, and effect of SPS on the adsorption of Pb(II) onto aged microplastics (mass: volume = 1 g/L) was shown in Fig. 9f. With the increasing concentration of SPS in the overall range of 0–500 mg/L, the total adsorption capacity of the binary systems of aged microplastics and SPS to Pb (II) rapidly increased. Nevertheless, compared with the control group containing only SPS particles, some interesting phenomenons about "1 + 1 < 2?" were observed in the the binary systems. The phenomenon might be explained by the fact that when the concentration of SPS exceeded a certain threshold value, Pb(II) contents adsorbed by the "aged microplastics + SPS" systems was lower than that in the separately superimposed adsorption amounts of both aged microplastics and SPS, except for TWP. The adsorption capacity of SPS at the 1, 10, 100 and 500 mg/L to Pb(II) was 0.31 ± 0.15, 0.31 ± 0.14, 2.83 ± 0.06 and 8.15 ± 0.14 mg/g, while the adsorption of TWP, UV-PLA and UV-PS without the addition of SPS was 0.89 ± 0.10, 0.70 ± 0.14 and 0.40 ± 0.16 mg/L, respecively. For the binary systems of UV-PS and SPS, unless the SPS concentration of 10 mg/L, their adsorption capacity was less than the sum of two single system and even lower than the single SPS system at 500 mg/L. For the binary systems of UV-PLA and SPS, their adsorption amounts were almost identical to the sum of two single system together when the SPS concentration < 10 mg/L. Subsequently, it was far less than superimposed adsorption amounts of both two systems and even lower than the single SPS system at the 500 mg/L. The result was similar to Guan et al. [89], who reported that in the sediment system composed of 200 mg SPS, pristine or aged microplastics (10 % w/w of SPS), Pb(II) ions and 50 mL solution environment, the high concentration of SPS exhibited the highest adsorption amounts of Pb(II), otherwise the addition of microplastics decreased the adsorption capacity especially UV-PLA due to the increase of Zeta potential. Inversely, adsorption capacity in the binary systems of TWP and SPS was significantly enhanced with the increase of SPS and greater than the the sum of two single adsorption system, indicating that the interactions between TWP and SPS had a synergistic effect about about "1 + 1 > 2" on the adsorption behavior of metal ions. These results implied that the impact of SPS particles on the metal adsorption by the "aged microplastics + SPS" binary system showed a concentration-dependent and polymer-dependent trend.

In order to further investigate the interactions between agd microplastics and SPS, "microplastics-sediment" combination mixtures were obtained by filtering the upper suspension in the binary system. Fig. 9f (1–4) compared the SEM images of SPS, "TWP-SPS", "UV-PLA-SPS" and "UV-PS-SPS" mixtures. In the mixed suspension of SPS and aged microplastics, the smaller SPS particles were absorbed and adhered on the surface of aged microplastics and both of heteroaggregates were formed due to the surface charges, electrostatic attraction and surface functional groups [45,90]. As shown in Fig. 9f(2), SPS preferred to adhere on the rougher surface of TWP and even a part of them were filled into the TWP pores. This phenomenon might explain that the stronger heterogeneous aggregation effect of TWP and SPS enhanced their adsorption ability to Pb(II) in the binary system. Besides, only a small amounts of SPS were attached to the surface of UV-PLA and UV-PS (Fig. 9f(3 and 4)). When the concentration of SPS was low, a minimal adhesion of SPS did not affect the adsorption capacity of binary systems; With the concentration of SPS higher than a certain threshold, their intensive interaction between SPS and aged microplastics (UV-PLA and UV-PS) might reduce the common adsorption sites to Pb(II) and meanwhile alter the surface electrostatic interaction, leading to the inhibiting effect about "1 + 1 < 2" and decreasing the adsorption capacity to metal ions compared with both of single adsorption systems. In summary, these findings suggested that SPS had the multiple effect on fate and transport of metal pollutants during the adsorption process of different aged microplastics.

3.6. Desorption behavior of Pb(II) from aged microplastics in the sediment and water column environments

The Pb(II) desorption behavior from three representative aged microplastics after reaching the Pb(II) adsorption equilibrium in two typical aquatic environments and the effects of environmental factors including HA and salinity were exhibited in Fig. 10. On the one hand, Fig. 10a showed that the desorption quantity in the simulated sediment environment was followed the order of Pb-laden UV-PLA > Pb-laden TWP > Pb-laden UV-PS, among which Pb-laden UV-PLA had the highest Pb(II) desorption capacity and far exceeded the other microplastics. In addition, the desorption quantity of Pb(II)-laden aged microplastics was changed in the presence of HA and salinity, presenting that HA inhibited the Pb(II) desorption from aged microplastics in the sediment environment, while salinity enhanced the Pb(II) desorption. Notably, whether the presence in the HA or salinity, the desorption capacity of Pb(II)-laden aged microplastics in the simulated sediment environment was still followed by Pb-laden UV-PLA, Pb-laden TWP and Pb-laden UV-PS, respectively. According to Fig. 10a and Table S9, Pb-laden UV-PLA in the sediment environment, sediment environment with HA and sediment environment with salinity among demonstrated the highest desorption efficiency and their desorption rates were 48.7 ± 5.43 %, 25.07 ± 11.37 % and 56.35 ± 5.86 %, respectively. Compared with Pb-laden UV-PLA, the desorption efficiency of Pb-laden TWP and Pb-laden UV-PS was relatively lower, showing that the desorption rates of Pb-laden TWP in the sediment environment, sediment environment with HA and sediment environment with salinity were 9.65 ± 1.28 %, 2.06 ± 0.47 % and 11.18 ± 1.21 %, while the Pb-laden UV-PS was 6.16 ± 0.95 %, 1.87 ± 0.53 %, 14.99 ± 3.34 %, respectively. In general, the objective pattern of Pb(II) desorption rate from three aged microplastics in the sediment systems was almost consistent with their Pb(II) desorption quantity, indicating the nonnegligible desorption risks of metal

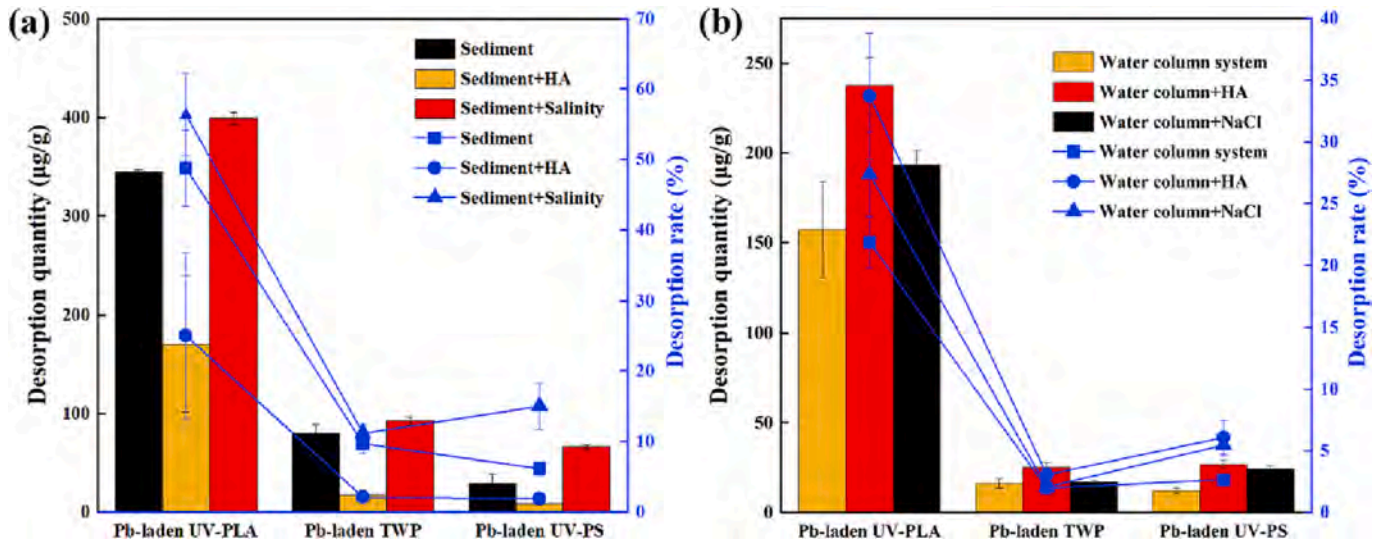

Fig. 10. Desorption quantity and rates of Pb(II) from three Pb-laden aged microplastics (TWP, UV-PLA and UV-PS) in the absence and presence of humic acid (HA, 10 mg/L) and salinity (NaCl, 50 mM) in the simulated (a) sediment environment and (b) turbulent water column.

pollutants from the biodegradable microplastics to various benthic organisms. Considering that PLA microplastics attached with metal contaminants can be exposed and ingested by benthic organisms, the bioavailability and combined toxicity of the metal contaminants and aged microplastics need to be evaluated [9].

On the other hand, Fig. 10b showed the Pb(II) desorption behavior of three Pb(II)-laden aged microplastics in the simulated turbulent water column. Among the three aged microplastics, Pb-laden UV-PLA has the highest Pb(II) desorption quantity, and subsequently, Pb-laden TWP and Pb-laden UV-PS had a similar desorption capacity. Furthermore, the desorption quantity of three aged microplastics can by affected by the presence of HA and salinity, both of which HA and salinity promoted the Pb(II) desorption in the turbulent aquatic column environment and the enhancement effect of HA was slightly greater than that of salinity. On the basis of Fig. 10b and Table S9, the desorption efficiency of Pb-laden UV-PLA in the water column environment, water column containing HA and water column containing salinity was 21.86 ± 2.06 %, 33.72 ± 5.10 % and 27.39 ± 3.43 %, respectively, which was far greater than that followed by the Pb-laden UV-PS and Pb-laden TWP. The desorption rates from Pb-laden UV-PS in water column environment, water column containing HA and water column containing salinity were 2.66 %, 6.09 % and 5.46 %, while the desorption rates from Pb-laden TWP were 1.98 %, 3.06 % and 2.06 %, respectively. Differed from the sediment system, both HA and salinity in the water column environments increased the Pb (II) desorption rates and the desorption efficiency of Pb-laden UV-PS was higher than Pb-laden TWP. In comparison, the Pb(II) desorption quantity and rates of different aged microplastics in sediment systems were significantly higher than those in turbulent water column systems, except for the aquatic situation containing HA. Reletively lower desorption rates were observed in the turbulent water column (Table S9), impling that the majority of adsorbed Pb(II) might be remained on the aged microplastics in water column systems.

Meanwhile, the Zn(II) leaching behavior of Pb-laden TWP in the desorption systems was investigated. The leaching amounts of Zn(II) from Pb-laden TWP in the in the sediment systems, sediment with HA and sediment with salinity were 397.08 ± 6.10, 323.13 ± 19.05 and 306.10 ± 28.74 μg/L, while it in the turbulent water column systems, water column containing HA and water column containing salinity were 150.93 ± 8.40, 143.44 ± 16.83 and 106.72 ± 3.67 μg/L, respectively. Notably, Zn(II) released more easily in the sediment environment than that in the turbulent water column, whereas the presence of salinity and HA in the two aquatic environment slightly inhibited the leaching of Zn (II) from the Pb-laden TWP. The leaching concentration of other metals (e.g., Cd(II), Co(II), Cu(II), Na(II), Mg(II), Ni(II)) was 0-several μg/L, which was almost similar to the the metal leaching system of TWP. Compared with the metal leaching system of TWP, these leaching amounts from two desorption systems in the presence or absence of salinity or HA significantly decreased, while Zn(II) can be released from TWP for a persistent and long-term period.

Basically, the migration and ecotoxicology of chemical contaminants are closely related to the desorption properties and ability. As shown in Table S10, knowledge about the desorption behavior of metal ions from aged microplastics remains limited. In general, the desorption capacity of chemical pollutants from microplastics was mainly determined by the strength of the interfacial binding force between microplastic surface and co-existing pollutants [62,91]. Additionally, the plastic composition and size, surface physical properties (e.g., Zeta potential) and functional groups in different types of microplastics are likely to affect the desorption behavior of environmental pollutants [41,92]. The aging process (e.g., UV aging, biofilm attachment) can increase the stability of contaminants on plastic surface, suppress the desorption ability of metal ions and make metal-laden aged microplastics more irreversible than pristine microplastics [28,92,93]. Overall, our findings showed that Pb (II) desorption quantity and rates from different aged microplastics in sediment system were generally higher than those in turbulent water column system. By the comparison between both of the sediment system and turbulent water column environment, biodegradable microplastics UV-PLA had the strongest desorption ability of Pb(II) than that of conventional UV-PS and their values of desorption ratio ranged from 21.86 to 56.35 % under the influence of environmental factors, potentially serving as an important vecor of metal pollutants into various aquatic environments and organism tissues and posing the considerable environmental risks. Therefore, biodegradable plastics, as a type of notional "green" and environemntally-friendly materials, should be reconsidered its potential environmental risks (e.g., the difficulty in rapid degradation, formation of micro/nanoplastics, vector for environmental pollutants, ecological toxicity) before the widespread application and popularzation around the world [15,19]. Moreover, the environmental factors (e.g., natural organic matter, salinity) can significantly affect the desorption capacity and rates of metal ions and cause the different inhibitory or promotive effects on the desorption behavior from aged microplastics, indicating that aquatic chemistry increased the complexity of the desorption process of Pb(II). Thus, various environmental factors must be take into consideration in the risks betweeen microplastics and metal pollutants. Although metal desorption rate of TWP was obviously weaker than that of UV-PLA, TWP still posed a

nonnegligible threat due to its largest adsorption ability to environmental pollutants and the complexity of released compounds (e.g., Zn (II), toxic organic pollutants). Similarly, limited studies also reported that biodegradable microplastics and TWP are likely to have the stronger desorption capacity of metal ions than the conventional microplastics. Liao and Yang [94] demonstrated that pristine PLA microplastics was more easier to desorb Cr(VI) and Cr(III) than the conventional microplastics (PE, PP, PVC, PS), leading to the highest Cr (VI) oral bioaccessibility in the human digestive systems. For the desorption behavior of TWP, Fan et al. [28] showed that the desorption quantity (0.60–3.08 mg/g) and desorption rate (10.85–75.73 %) of Cd (II) and Pb(II) from UV-TWP and pristine TWP in the simulated human gastric fluid environment were significantly higher than that from the conventional UV-PP and pristine PP. The UV aging significantly decreased the desorption rate of metal ions from TWP and PP due to the stronger bonding strength and increase of oxygen-containing functional groups. Generally, the desorption amounts of environmental contaminants from microplastics in the simulated intestinal fluid was greater than that in sole aquatic environments, suggesting the "carrier" effect of aged microplastics and a considerable health risk of absorbing or leaching pollutants into various aquatic organisms and even human (Table S10). Meanwhile, further exploration should be continue to the impact mechanisms and potential ecological effects by biodegradable microplastics and TWP due to its greater adsorption and desorption ability than that of conventional microplastics.

4. Conclusion

In this work, the environmentally-relevant TWP had the greatest adsorption ability and was followed by UV-PLA, UV-PS, PLA and PS, with the considerable concern about the impacts of natural aging behavior and multifarious environmental factors. The release kinetics of Zn(II) from TWP and its impact on the metal ion adsorption/desorption remained more investigation. Aging/weathering behavior, considered as a type of strong environmental stress, significantly changed the physicochemical properties of microplastics and further promoted their adsorption capacity to Pb(II). The aging evaluation of physicochemical properties to microplastics showed that the rougher surface, larger specific surface area and pore volume, smaller particle size and negative Zeta potential responded to the greater adsorption capacity of the UV-PLA and UV-PS than pristine microplastics, and the increase of surface oxygen-containing functional groups were verified by the variation of carbonyl index and oxygen/carbon ratio, especially for UV-PLA. The electrostatic interaction and complexation of oxygen-containing functional groups played vital roles in the adsorption mechanism of Pb(II) onto the biodegradable and conventional microplastics, cation-π interaction could be relevant to the adsorption of UV-PS, while the adsorption mechanism of TWP with a relatively poor physical properties was largely determined by the complexation of surface functional groups and properties of the complex co-polymer itself. Moreover, the environmental factors such as pH, natural organic matter, salinity, surfactant, coexisting Cu(II) and SPS markedly affected Pb(II) adsorption capacity of aged microplastics in varying degrees, among which HA and SPS had the greatest influence. The adsorption capacity of Pb(II) onto aged microplastics gradually promoted with the increase of pH, surfactant SDS and salinity, but the coexisting Cu(II) generally inhibited adsorption capacity of Pb(II). HA, as a typical natural organic matters that can bind to both microplastics and metal ions, had a dual effect to the adsorption process of microplastics. The hetero-aggregates formed by SPS and microplastics varied with the types of microplastics, which might be the reason for the concentration-dependent and polymer-dependent trend of the Pb(II) adsorption capacity onto different binary systems. Additionally, desorption quantity and rates of Pb(II) from UV-PLA both in the simulated sediment environment and turbulent water column were far beyond than that of TWP and UV-PS. The desorption ability of TWP and UV-PS varied from the two kinds of aquatic environments and relevant environmental factors (e.g., HA and salinity). In conclusion, this work has significant environmental implications for understanding the vector effect, fate and risk assessment of aged microplastics especially TWP and biodegradable microplastics.

Declaration of Competing Interest

The authors declare that they have no known competing financial interests or personal relationships that could have appeared to influence the work reported in this paper.

Data availability

Data will be made available on request.

Acknowledgements

This study was supported by the Program for the National Natural Science Foundation of China (Grant 52039001, 51521006, 51979101, 52100185) and the BNU Interdisciplinary Research Foundation for the First-Year Doctoral Candidates (Grant BNUXKJC2117). We sincerely thank the Dr. Hongjie Tang and Dr. Xi Hu from the Quantum Design Co., Ltd (Beijing, China) for the O-PTIR analysis.

Appendix A. Supplementary data

Supplementary data to this article can be found online at https://doi.org/10.1016/j.cej.2023.141838.

References

[1] Plastics*Europe*, Plastics - the Facts 2020. An analysis of European plastics production, demand and waste data, 2021.
[2] R. Geyer, J.R. Jambeck, K.L. Law, Production, use, and fate of all plastics ever made, Sci. Adv. 3 (7) (2017) e1700782.
[3] C. Arthur, J.E. Baker, H.A. Bamford, Proceedings of the International Research Workshop on the Occurrence, Effects, and Fate of Microplastic Marine Debris, University of Washington Tacoma, Tacoma, WA, USA, 2009.
[4] P. Liu, X. Zhan, X. Wu, J. Li, H. Wang, S. Gao, Effect of weathering on environmental behavior of microplastics: Properties, sorption and potential risks, Chemosphere 242 (2020), 125193, https://doi.org/10.1016/j.chemosphere.2019.125193.
[5] J.P. McDevitt, C.S. Criddle, M. Morse, R.C. Hale, C.B. Bott, C.M. Rochman, Addressing the issue of microplastics in the wake of the microbead-free waters act—A new standard can facilitate improved policy, Environ. Sci. Tech. 51 (12) (2017) 6611–6617, https://doi.org/10.1021/acs.est.6b05812.
[6] B. Xue, L. Zhang, R. Li, Y. Wang, J. Guo, K. Yu, S. Wang, Underestimated microplastic pollution derived from fishery activities and "hidden" in deep sediment, Environ. Sci. Tech. 54 (4) (2020) 2210–2217, https://doi.org/10.1021/acs.est.9b04850.
[7] M.S. Bank, S.V. Hansson, The plastic cycle: A novel and holistic paradigm for the anthropocene, Environ. Sci. Tech. 53 (13) (2019) 7177–7179, https://doi.org/10.1021/acs.est.9b02942.
[8] W. Huang, M. Chen, B. Song, J. Deng, M. Shen, Q. Chen, G. Zeng, J. Liang, Microplastics in the coral reefs and their potential impacts on corals: A mini-review, Sci. Total Environ. 762 (2021), 143112, https://doi.org/10.1016/j.scitotenv.2020.143112.
[9] W. Huang, B. Song, J. Liang, Q. Niu, G. Zeng, M. Shen, J. Deng, Y. Luo, X. Wen, Y. Zhang, Microplastics and associated contaminants in the aquatic environment: A review on their ecotoxicological effects, trophic transfer, and potential impacts to human health, J. Hazard. Mater. 405 (2021), 124187, https://doi.org/10.1016/j.jhazmat.2020.124187.
[10] C.M. Rochman, C. Brookson, J. Bikker, N. Djuric, A. Earn, K. Bucci, S. Athey, A. Huntington, H. McIlwraith, K. Munno, H. De Frond, A. Kolomijeca, L. Erdle, J. Grbic, M. Bayoumi, S.B. Borrelle, T. Wu, S. Santoro, L.M. Werbowski, X. Zhu, R. K. Giles, B.M. Hamilton, C. Thaysen, A. Kaura, N. Klasios, L. Ead, J. Kim, C. Sherlock, A. Ho, C. Hung, Rethinking microplastics as a diverse contaminant suite, Environ. Toxicol. Chem. 38 (4) (2019) 703–711, https://doi.org/10.1002/etc.4371.
[11] S.A. Ashter, Introduction, in: S.A. Ashter (Ed.), Introduction to Bioplastics Engineering, William Andrew Publishing, Oxford, 2016, pp. 1–17,, https://doi.org/10.1016/B978-0-323-39396-6.00001-4.
[12] E. Bioplastics, Bioplastics Market Data 2020, in: E. Bioplastics (Ed.) European Bioplastics, 2020.
[13] T.P. Haider, C. Völker, J. Kramm, K. Landfester, F.R. Wurm, Plastics of the future? The impact of biodegradable polymers on the environment and on society, Angew. Chem. Int. Ed. 58 (1) (2019) 50–62, https://doi.org/10.1002/anie.201805766.

[14] S. Lambert, M. Wagner, Environmental performance of bio-based and biodegradable plastics: the road ahead, Chem. Soc. Rev. 46 (22) (2017) 6855–6871, https://doi.org/10.1039/C7CS00149E.
[15] X.-F. Wei, M. Bohlén, C. Lindblad, M. Hedenqvist, A. Hakonen, Microplastics generated from a biodegradable plastic in freshwater and seawater, Water Res. 198 (2021), 117123, https://doi.org/10.1016/j.watres.2021.117123.
[16] M. González-Pleiter, M. Tamayo-Belda, G. Pulido-Reyes, G. Amariei, F. Leganés, R. Rosal, F. Fernández-Piñas, Secondary nanoplastics released from a biodegradable microplastic severely impact freshwater environments, Environ. Sci. Nano 6 (5) (2019) 1382–1392, https://doi.org/10.1039/c8en01427b.
[17] J. Liao, Q. Chen, Biodegradable plastics in the air and soil environment: Low degradation rate and high microplastics formation, J. Hazard. Mater. 418 (2021), 126329, https://doi.org/10.1016/j.jhazmat.2021.126329.
[18] D.S. Green, B. Boots, N.E. O'Connor, R. Thompson, Microplastics Affect the Ecological Functioning of an Important Biogenic Habitat, Environ. Sci. Tech. 51 (1) (2017) 68–77, https://doi.org/10.1021/acs.est.6b04496.
[19] K. Klein, T. Piana, T. Lauschke, P. Schweyen, G. Dierkes, T. Ternes, U. Schulte-Oehlmann, J. Oehlmann, Chemicals associated with biodegradable microplastic drive the toxicity to the freshwater oligochaete Lumbriculus variegatus, Aquat. Toxicol. 231 (2021), 105723, https://doi.org/10.1016/j.aquatox.2020.105723.
[20] X. Zhang, M. Xia, X. Su, P. Yuan, X. Li, C. Zhou, Z. Wan, W. Zou, Photolytic degradation elevated the toxicity of polylactic acid microplastics to developing zebrafish by triggering mitochondrial dysfunction and apoptosis, J. Hazard. Mater. 413 (2021), 125321, https://doi.org/10.1016/j.jhazmat.2021.125321.
[21] G. Malafaia, Í.F. Nascimento, F.N. Estrela, A.T.B. Guimarães, F. Ribeiro, T.M.d. Luz, A.S.d.L. Rodrigues, Green toxicology approach involving polylactic acid biomicroplastics and neotropical tadpoles: (Eco)toxicological safety or environmental hazard? Sci. Total Environ. 783 (2021) 146994, https://doi.org/10.1016/j.scitotenv.2021.146994.
[22] S. Wagner, T. Hüffer, P. Klöckner, M. Wehrhahn, T. Hofmann, T. Reemtsma, Tire wear particles in the aquatic environment - A review on generation, analysis, occurrence, fate and effects, Water Res. 139 (2018) 83–100, https://doi.org/10.1016/j.watres.2018.03.051.
[23] N.B. Hartmann, T. Huffer, R.C. Thompson, M. Hassellov, A. Verschoor, A. E. Daugaard, S. Rist, T. Karlsson, N. Brennholt, M. Cole, M.P. Herrling, M.C. Hess, N.P. Ivleva, A.L. Lusher, M. Wagner, Are we speaking the same language? Recommendations for a definition and categorization framework for plastic debris, Environ. Sci. Tech. 53 (3) (2019) 1039–1047, https://doi.org/10.1021/acs.est.8b05297.
[24] P. Klöckner, B. Seiwert, P. Eisentraut, U. Braun, T. Reemtsma, S. Wagner, Characterization of tire and road wear particles from road runoff indicates highly dynamic particle properties, Water Res. 185 (2020), 116262, https://doi.org/10.1016/j.watres.2020.116262.
[25] P.E. Redondo-Hasselerharm, V.N. de Ruijter, S.M. Mintenig, A. Verschoor, A. A. Koelmans, Ingestion and chronic effects of car tire tread particles on freshwater benthic macroinvertebrates, Environ. Sci. Tech. 52 (23) (2018) 13986–13994, https://doi.org/10.1021/acs.est.8b05035.
[26] A. Kolomijeca, J. Parrott, H. Khan, K. Shires, S. Clarence, C. Sullivan, L. Chibwe, D. Sinton, C.M. Rochman, Increased temperature and turbulence alter the effects of leachates from tire particles on fathead minnow (pimephales promelas), Environ. Sci. Tech. 54 (3) (2020) 1750–1759, https://doi.org/10.1021/acs.est.9b05994.
[27] M. Capolupo, L. Sørensen, K.D.R. Jayasena, A.M. Booth, E. Fabbri, Chemical composition and ecotoxicity of plastic and car tire rubber leachates to aquatic organisms, Water Res. 169 (2020), 115270, https://doi.org/10.1016/j.watres.2019.115270.
[28] X. Fan, Z. Ma, Y. Zou, J. Liu, J. Hou, Investigation on the adsorption and desorption behaviors of heavy metals by tire wear particles with or without UV ageing processes, Environ. Res. 195 (2021), 110858, https://doi.org/10.1016/j.envres.2021.110858.
[29] X. Fan, R. Gan, J. Liu, Y. Xie, D. Xu, Y. Xiang, J. Su, Z. Teng, J. Hou, Adsorption and desorption behaviors of antibiotics by tire wear particles and polyethylene microplastics with or without aging processes, Sci. Total Environ. 771 (2021), 145451, https://doi.org/10.1016/j.scitotenv.2021.145451.
[30] D. Brennecke, B. Duarte, F. Paiva, I. Caçador, J. Canning-Clode, Microplastics as vector for heavy metal contamination from the marine environment, Estuar. Coast. Shelf Sci. 178 (2016) 189–195, https://doi.org/10.1016/j.ecss.2015.12.003.
[31] D.J. Sarkar, S. Das Sarkar, B.K. Das, B.K. Sahoo, A. Das, S.K. Nag, R.K. Manna, B. K. Behera, S. Samanta, Occurrence, fate and removal of microplastics as heavy metal vector in natural wastewater treatment wetland system, Water Res. 192 (2021), 116853, https://doi.org/10.1016/j.watres.2021.116853.
[32] J. Guan, K. Qi, J. Wang, W. Wang, Z. Wang, N. Lu, J. Qu, Microplastics as an emerging anthropogenic vector of trace metals in freshwater: Significance of biofilms and comparison with natural substrates, Water Res. 184 (2020), 116205, https://doi.org/10.1016/j.watres.2020.116205.
[33] H. Luo, C. Liu, D. He, J. Xu, J. Sun, J. Li, X. Pan, Environmental behaviors of microplastics in aquatic systems: A systematic review on degradation, adsorption, toxicity and biofilm under aging conditions, J. Hazard. Mater. 423 (2022), 126915, https://doi.org/10.1016/j.jhazmat.2021.126915.
[34] C.C. Chen, X. Zhu, H. Xu, F. Chen, J. Ma, K. Pan, Copper adsorption to microplastics and natural particles in seawater: A comparison of kinetics, isotherms, and bioavailability, Environ. Sci. Tech. 55 (20) (2021) 13923–13931, https://doi.org/10.1021/acs.est.1c04278.
[35] J. Duan, N. Bolan, Y. Li, S. Ding, T. Atugoda, M. Vithanage, B. Sarkar, D.C. W. Tsang, M.B. Kirkham, Weathering of microplastics and interaction with other coexisting constituents in terrestrial and aquatic environments, Water Res. 196 (2021), 117011, https://doi.org/10.1016/j.watres.2021.117011.
[36] M. Carbery, G.R. MacFarlane, W. O'Connor, S. Afrose, H. Taylor, T. Palanisami, Baseline analysis of metal(loid)s on microplastics collected from the Australian shoreline using citizen science, Mar. Pollut. Bull. 152 (2020), 110914, https://doi.org/10.1016/j.marpolbul.2020.110914.
[37] A.I.S. Purwiyanto, Y. Suteja, Trisno, P.S. Ningrum, W.A.E. Putri, Rozirwan, F. Agustriani, Fauziyah, M.R. Cordova, A.F. Koropitan, Concentration and adsorption of Pb and Cu in microplastics: Case study in aquatic environment, Mar. Pollut. Bull. 158 (2020) 111380, https://doi.org/10.1016/j.marpolbul.2020.111380.
[38] V. Godoy, G. Blázquez, M. Calero, L. Quesada, M.A. Martín-Lara, The potential of microplastics as carriers of metals, Environ. Pollut. 255 (2019), 113363, https://doi.org/10.1016/j.envpol.2019.113363.
[39] Q. Li, J. Wu, X. Zhao, X. Gu, R. Ji, Separation and identification of microplastics from soil and sewage sludge, Environ. Pollut. 254 (2019), 113076, https://doi.org/10.1016/j.envpol.2019.113076.
[40] F.G. Torres, D.C. Dioses-Salinas, C.I. Pizarro-Ortega, G.E. De-la-Torre, Sorption of chemical contaminants on degradable and non-degradable microplastics: Recent progress and research trends, Sci. Total Environ. 757 (2021), 143875, https://doi.org/10.1016/j.scitotenv.2020.143875.
[41] Y. Zhou, Y. Yang, G. Liu, G. He, W. Liu, Adsorption mechanism of cadmium on microplastics and their desorption behavior in sediment and gut environments: The roles of water pH, lead ions, natural organic matter and phenanthrene, Water Res. 184 (2020), 116209, https://doi.org/10.1016/j.watres.2020.116209.
[42] J. Li, K. Zhang, H. Zhang, Adsorption of antibiotics on microplastics, Environ. Pollut. 237 (2018) 460–467, https://doi.org/10.1016/j.envpol.2018.02.050.
[43] Y. Xiong, J. Zhao, L. Li, Y. Wang, X. Dai, F. Yu, J. Ma, Interfacial interaction between micro/nanoplastics and typical PPCPs and nanoplastics removal via electrosorption from an aqueous solution, Water Res. 184 (2020), 116100, https://doi.org/10.1016/j.watres.2020.116100.
[44] Y. Jiang, X. Yin, X. Xi, D. Guan, H. Sun, N. Wang, Effect of surfactants on the transport of polyethylene and polypropylene microplastics in porous media, Water Res. 196 (2021), 117016, https://doi.org/10.1016/j.watres.2021.117016.
[45] Y. Li, X. Wang, W. Fu, X. Xia, C. Liu, J. Min, W. Zhang, J.C. Crittenden, Interactions between nano/micro plastics and suspended sediment in water: Implications on aggregation and settling, Water Res. 161 (2019) 486–495, https://doi.org/10.1016/j.watres.2019.06.018.
[46] J. Bhagat, N. Nishimura, Y. Shimada, Toxicological interactions of microplastics/nanoplastics and environmental contaminants: Current knowledge and future perspectives, J. Hazard. Mater. 405 (2021), 123913, https://doi.org/10.1016/j.jhazmat.2020.123913.
[47] S. Coffin, G.-Y. Huang, I. Lee, D. Schlenk, Fish and seabird gut conditions enhance desorption of estrogenic chemicals from commonly-ingested plastic items, Environ. Sci. Tech. 53 (8) (2019) 4588–4599, https://doi.org/10.1021/acs.est.8b07140.
[48] K. Zhu, H. Jia, Y. Sun, Y. Dai, C. Zhang, X. Guo, T. Wang, L. Zhu, Long-term phototransformation of microplastics under simulated sunlight irradiation in aquatic environments: Roles of reactive oxygen species, Water Res. 173 (2020), 115564, https://doi.org/10.1016/j.watres.2020.115564.
[49] R. Mao, M. Lang, X. Yu, R. Wu, X. Yang, X. Guo, Aging mechanism of microplastics with UV irradiation and its effects on the adsorption of heavy metals, J. Hazard. Mater. 393 (2020), 122515, https://doi.org/10.1016/j.jhazmat.2020.122515.
[50] Y. Su, X. Hu, H. Tang, K. Lu, H. Li, S. Liu, B. Xing, R. Ji, Steam disinfection releases micro(nano)plastics from silicone-rubber baby teats as examined by optical photothermal infrared microspectroscopy, Nat. Nanotechnol. 17 (1) (2022) 76–85, https://doi.org/10.1038/s41565-021-00998-x.
[51] S. Tang, L. Lin, X. Wang, A. Feng, A. Yu, Pb(II) uptake onto nylon microplastics: Interaction mechanism and adsorption performance, J. Hazard. Mater. 386 (2020), 121960, https://doi.org/10.1016/j.jhazmat.2019.121960.
[52] X. Xia, Z. Yang, X. Zhang, Effect of Suspended-Sediment Concentration on Nitrification in River Water: Importance of Suspended Sediment−Water Interface, Environ. Sci. Tech. 43 (10) (2009) 3681–3687, https://doi.org/10.1021/es8036675.
[53] B. Gewert, M.M. Plassmann, M. MacLeod, Pathways for degradation of plastic polymers floating in the marine environment, Environ. Sci. Processes Impacts 17 (9) (2015) 1513–1521, https://doi.org/10.1039/C5EM00207A.
[54] L. Gao, D. Fu, J. Zhao, W. Wu, Z. Wang, Y. Su, L. Peng, Microplastics aged in various environmental media exhibited strong sorption to heavy metals in seawater, Mar. Pollut. Bull. 169 (2021), 112480, https://doi.org/10.1016/j.marpolbul.2021.112480.
[55] C. Chen, F. Wei, L. Ye, Y. Wang, L. Long, C. Xu, Y. Xiao, J. Wu, M. Xu, J. He, G. Yang, Adsorption of Cu2+ by UV aged polystyrene in aqueous solution, Ecotoxicol. Environ. Saf. 232 (2022), 113292, https://doi.org/10.1016/j.ecoenv.2022.113292.
[56] K. Zhu, H. Jia, S. Zhao, T. Xia, X. Guo, T. Wang, L. Zhu, Formation of Environmentally Persistent Free Radicals on Microplastics under Light Irradiation, Environ. Sci. Tech. 53 (14) (2019) 8177–8186, https://doi.org/10.1021/acs.est.9b01474.
[57] Y.K. Song, S.H. Hong, M. Jang, G.M. Han, S.W. Jung, W.J. Shim, Combined effects of UV exposure duration and mechanical abrasion on microplastic fragmentation by polymer type, Environ. Sci. Tech. 51 (8) (2017) 4368–4376, https://doi.org/10.1021/acs.est.6b06155.
[58] P. Liu, L. Qian, H. Wang, X. Zhan, K. Lu, C. Gu, S. Gao, New insights into the aging behavior of microplastics accelerated by advanced oxidation processes, Environ. Sci. Tech. 53 (7) (2019) 3579–3588, https://doi.org/10.1021/acs.est.9b00493.
[59] L.L. Halle, A. Palmqvist, K. Kampmann, F.R. Khan, Ecotoxicology of micronized tire rubber: Past, present and future considerations, Sci. Total Environ. 706 (2020), 135694, https://doi.org/10.1016/j.scitotenv.2019.135694.

[60] J.K. McIntyre, J. Prat, J. Cameron, J. Wetzel, E. Mudrock, K.T. Peter, Z. Tian, C. Mackenzie, J. Lundin, J.D. Stark, K. King, J.W. Davis, E.P. Kolodziej, N.L. Scholz, Treading water: tire wear particle leachate recreates an urban runoff mortality syndrome in Coho but Not Chum Salmon, Environ. Sci. Tech. 55 (17) (2021) 11767–11774, https://doi.org/10.1021/acs.est.1c03569.
[61] A. Yu, X. Sun, S. Tang, Y. Zhang, M. Li, X. Wang, Adsorption mechanism of cadmium on polystyrene microplastics containing hexabromocyclododecane, Environ. Technol. Innov. 24 (2021), 102036, https://doi.org/10.1016/j.eti.2021.102036.
[62] Y. Wang, X. Wang, Y. Li, J. Li, F. Wang, S. Xia, J. Zhao, Biofilm alters tetracycline and copper adsorption behaviors onto polyethylene microplastics, Chem. Eng. J. 392 (2020), 123808, https://doi.org/10.1016/j.cej.2019.123808.
[63] J. Deng, X. Li, Y. Liu, G. Zeng, J. Liang, B. Song, X. Wei, Alginate-modified biochar derived from Ca(II)-impregnated biomass: Excellent anti-interference ability for Pb (II) removal, Ecotoxicol. Environ. Saf. 165 (2018) 211–218, https://doi.org/10.1016/j.ecoenv.2018.09.013.
[64] H. Zhang, J. Wang, B. Zhou, Y. Zhou, Z. Dai, Q. Zhou, P. Chriestie, Y. Luo, Enhanced adsorption of oxytetracycline to weathered microplastic polystyrene: Kinetics, isotherms and influencing factors, Environ. Pollut. 243 (2018) 1550–1557, https://doi.org/10.1016/j.envpol.2018.09.122.
[65] A.C. Martins, O. Pezoti, A.L. Cazetta, K.C. Bedin, D.A.S. Yamazaki, G.F.G. Bandoch, T. Asefa, J.V. Visentainer, V.C. Almeida, Removal of tetracycline by NaOH-activated carbon produced from macadamia nut shells: Kinetic and equilibrium studies, Chem. Eng. J. 260 (2015) 291–299, https://doi.org/10.1016/j.cej.2014.09.017.
[66] Y. Sun, X. Wang, S. Xia, J. Zhao, Cu(II) adsorption on Poly(Lactic Acid) Microplastics: Significance of microbial colonization and degradation, Chem. Eng. J. 429 (2022), 132306, https://doi.org/10.1016/j.cej.2021.132306.
[67] X. Fan, Y. Zou, N. Geng, J. Liu, J. Hou, D. Li, C. Yang, Y. Li, Investigation on the adsorption and desorption behaviors of antibiotics by degradable MPs with or without UV ageing process, J. Hazard. Mater. 401 (2021), 123363, https://doi.org/10.1016/j.jhazmat.2020.123363.
[68] F.-F. Liu, G.-Z. Liu, Z.-L. Zhu, S.-C. Wang, F.-F. Zhao, Interactions between microplastics and phthalate esters as affected by microplastics characteristics and solution chemistry, Chemosphere 214 (2019) 688–694, https://doi.org/10.1016/j.chemosphere.2018.09.174.
[69] O.S. Alimi, J. Farner Budarz, L.M. Hernandez, N. Tufenkji, Microplastics and Nanoplastics in Aquatic Environments: Aggregation, Deposition, and Enhanced Contaminant Transport, Environ. Sci. Technol., 52(4) (2018), pp. 1704-1724. 10.1021/acs.est.7b05559.
[70] Y. Xia, T. Yang, N. Zhu, D. Li, Z. Chen, Q. Lang, Z. Liu, W. Jiao, Enhanced adsorption of Pb(II) onto modified hydrochar: Modeling and mechanism analysis, Bioresour. Technol. 288 (2019), 121593, https://doi.org/10.1016/j.biortech.2019.121593.
[71] X. Colom, A. Faliq, K. Formela, J. Cañavate, FTIR spectroscopic and thermogravimetric characterization of ground tyre rubber devulcanized by microwave treatment, Polym. Test. 52 (2016) 200–208, https://doi.org/10.1016/j.polymertesting.2016.04.020.
[72] S. Gunasekaran, R.K. Natarajan, A. Kala, FTIR spectra and mechanical strength analysis of some selected rubber derivatives, Spectrochim. Acta A Mol. Biomol. Spectrosc. 68 (2) (2007) 323–330, https://doi.org/10.1016/j.saa.2006.11.039.
[73] M. Kovochich, J.A. Parker, S.C. Oh, J.P. Lee, S. Wagner, T. Reemtsma, K.M. Unice, Characterization of individual tire and road wear particles in environmental road dust, tunnel dust, and sediment, Environ. Sci. Technol. Lett. 8 (12) (2021) 1057–1064, https://doi.org/10.1021/acs.estlett.1c00811.
[74] M.E. Nolasco, V.A.S. Lemos, G. López, S.A. Soares, J.P.M. Feitosa, B.S. Araújo, A. P. Ayala, M.M.F. de Azevedo, F.E.P. Santos, R.M. Cavalcante, Morphology, chemical characterization and sources of microplastics in a coastal city in the equatorial zone with diverse anthropogenic activities (Fortaleza city, Brazil), J. Polym. Environ. 30 (7) (2022) 2862–2874, https://doi.org/10.1007/s10924-022-02405-5.
[75] F. Karabork, E. Pehlivan, A. Akdemir, Characterization of styrene butadiene rubber and microwave devulcanized ground tire rubber composites, J. Polym. Eng. 34 (6) (2014) 543–554, https://doi.org/10.1515/polyeng-2013-0330.
[76] Q. Wang, Y. Zhang, Y. Zhang, Z. Liu, J. Wang, H. Chen, Effects of biofilm on metal adsorption behavior and microbial community of microplastics, J. Hazard. Mater. 424 (2022), 127340, https://doi.org/10.1016/j.jhazmat.2021.127340.
[77] W.-H. Lin, J. Kuo, S.-L. Lo, Effect of light irradiation on heavy metal adsorption onto microplastics, Chemosphere 285 (2021), 131457, https://doi.org/10.1016/j.chemosphere.2021.131457.
[78] X. Wu, P. Liu, Z. Gong, H. Wang, H. Huang, Y. Shi, X. Zhao, S. Gao, Humic acid and fulvic acid hinder long-term weathering of microplastics in lake water, Environ. Sci. Tech. 55 (23) (2021) 15810–15820, https://doi.org/10.1021/acs.est.1c04501.
[79] W. Chen, Z.-Y. Ouyang, C. Qian, H.-Q. Yu, Induced structural changes of humic acid by exposure of polystyrene microplastics: A spectroscopic insight, Environ. Pollut. 233 (2018) 1–7, https://doi.org/10.1016/j.envpol.2017.10.027.
[80] X. Li, Q. Mei, L. Chen, H. Zhang, B. Dong, X. Dai, C. He, J. Zhou, Enhancement in adsorption potential of microplastics in sewage sludge for metal pollutants after the wastewater treatment process, Water Res. 157 (2019) 228–237, https://doi.org/10.1016/j.watres.2019.03.069.
[81] S. Tang, L. Lin, X. Wang, X. Sun, A. Yu, Adsorption of fulvic acid onto polyamide 6 microplastics: Influencing factors, kinetics modeling, site energy distribution and interaction mechanisms, Chemosphere 272 (2021), 129638, https://doi.org/10.1016/j.chemosphere.2021.129638.
[82] A.A. Siyal, M.R. Shamsuddin, A. Low, N.E. Rabat, A review on recent developments in the adsorption of surfactants from wastewater, J. Environ. Manage. 254 (2020), 109797, https://doi.org/10.1016/j.jenvman.2019.109797.
[83] Y. Jiang, S. Zhou, J. Fei, Z. Qin, X. Yin, H. Sun, Y. Sun, Transport of different microplastics in porous media: Effect of the adhesion of surfactants on microplastics, Water Res. 215 (2022), 118262, https://doi.org/10.1016/j.watres.2022.118262.
[84] B.S. Rauniyar, A. Bhattarai, Study of conductivity, contact angle and surface free energy of anionic (SDS, AOT) and cationic (CTAB) surfactants in water and isopropanol mixture, J. Mol. Liq. 323 (2021), 114604, https://doi.org/10.1016/j.molliq.2020.114604.
[85] W. Zhang, L. Zhang, T. Hua, Y. Li, X. Zhou, W. Wang, Z. You, H. Wang, M. Li, The mechanism for adsorption of Cr(VI) ions by PE microplastics in ternary system of natural water environment, Environ. Pollut. 257 (2020), 113440, https://doi.org/10.1016/j.envpol.2019.113440.
[86] X. Huang, D.Y. Zemlyanov, S. Diaz-Amaya, M. Salehi, L. Stanciu, A.J. Whelton, Competitive heavy metal adsorption onto new and aged polyethylene under various drinking water conditions, J. Hazard. Mater. 385 (2020), 121585, https://doi.org/10.1016/j.jhazmat.2019.121585.
[87] M. Besson, H. Jacob, F. Oberhaensli, A. Taylor, P.W. Swarzenski, M. Metian, Preferential adsorption of Cd, Cs and Zn onto virgin polyethylene microplastic versus sediment particles, Mar. Pollut. Bull. 156 (2020), 111223, https://doi.org/10.1016/j.marpolbul.2020.111223.
[88] X. Wang, R. Zhang, Z. Li, B. Yan, Adsorption properties and influencing factors of Cu(II) on polystyrene and polyethylene terephthalate microplastics in seawater, Sci. Total Environ. 812 (2022), 152573, https://doi.org/10.1016/j.scitotenv.2021.152573.
[89] Y. Guan, J. Gong, B. Song, J. Li, S. Fang, S. Tang, W. Cao, Y. Li, Z. Chen, J. Ye, Z. Cai, The effect of UV exposure on conventional and degradable microplastics adsorption for Pb (II) in sediment, Chemosphere 286 (2022), 131777, https://doi.org/10.1016/j.chemosphere.2021.131777.
[90] Y. Zhang, Y. Luo, X. Guo, T. Xia, T. Wang, H. Jia, L. Zhu, Charge mediated interaction of polystyrene nanoplastic (PSNP) with minerals in aqueous phase, Water Res. 178 (2020), 115861, https://doi.org/10.1016/j.watres.2020.115861.
[91] S. Zhang, B. Han, Y. Sun, F. Wang, Microplastics influence the adsorption and desorption characteristics of Cd in an agricultural soil, J. Hazard. Mater. 388 (2020), 121775, https://doi.org/10.1016/j.jhazmat.2019.121775.
[92] M.D. Sharma, R.J. Krupadam, Adsorption-desorption dynamics of synthetic and naturally weathered microfibers with toxic heavy metals and their ecological risk in an estuarine ecosystem, Environ. Res. 207 (2022), 112198, https://doi.org/10.1016/j.envres.2021.112198.
[93] Y. Wang, X. Wang, Y. Li, J. Li, Y. Liu, S. Xia, J. Zhao, Effects of exposure of polyethylene microplastics to air, water and soil on their adsorption behaviors for copper and tetracycline, Chem. Eng. J. 404 (2021), 126412, https://doi.org/10.1016/j.cej.2020.126412.
[94] Y.-L. Liao, J.-Y. Yang, Microplastic serves as a potential vector for Cr in an in-vitro human digestive model, Sci. Total Environ. 703 (2020), 134805, https://doi.org/10.1016/j.scitotenv.2019.134805.